UNIVERSIDADE DE LISBOA
FACULDADE DE CIÊNCIAS
DEPARTAMENTO DE QUÍMICA E BIOQUÍMICA

Structural and conformational effects of metal binding to the S100B cytokine

Sofia Baptista de Carvalho

Mestrado em Bioquímica
2011

UNIVERSIDADE DE LISBOA
FACULDADE DE CIÊNCIAS
DEPARTAMENTO DE QUÍMICA E BIOQUÍMICA

Structural and conformational effects of metal binding to the S100B cytokine

Sofia Baptista de Carvalho
Tese orientada por Doutor Cláudio M. Gomes (ITQB-UNL) e
Doutora Ana A. Coutinho (FC-UL)

Mestrado em Bioquímica
2011

Foreword

This dissertation describes the work performed under the supervision of Dr. Cláudio M. Gomes, in the Protein Biochemistry Folding and Stability Laboratory, at the Instituto de Tecnologia Química e Biológica, from September 2010 to September 2011.

The studies presented here aim at understanding the role of metal ions such as Ca^{2+}, Cu^{2+} and Zn^{2+}, in conformation and stability of S100B cytokine. It intends to clarify also the metal-dependent mechanisms through which the structure and biological function of S100B protein occurs.

The thesis is organized in four parts. The first chapter presents the state of the art on fundamental aspects of protein folding, metal ions in biology and their interplay. Moreover, it presents an overview of S100 proteins and in particular S100B, the system in study. The following chapter includes an overview of the biophysical methods used to monitor protein conformational stability and also the procedures performed during this work. The third chapter reports the main experimental results obtained in the study of S100B conformation and stability modulation by metal ions. The last chapter highlights the general conclusions of the described results and future perspectives.

Abstract

S100B is a Ca^{2+}, Cu^{2+} and Zn^{2+}-binding protein highly expressed in human brain, with a intra and extracellular function. It is involved in several pathological processes in which metal homeostasis is imbalanced, such as AD and ALS, which account for a modified protein function. Metal binding to S100B induces conformational changes. However, the mechanisms underlying this modulation and how it affects protein stability remain uncharacterized. Here, we extensively address the effects of metal binding on the folding and stability of S100B. The physiological environment in which S100B accumulates, such as the synaptic cleft, is metal ion rich so the protein–metal interplay is relevant to understand S100B physiological (and pathophysiological) role. With this purpose we have studied the native form of human S100B as well as a Cys-to-Ser mutated variant, S100B ΔCys, which abolishes metal bonding.

Our results showed that Cu^{2+} and Zn^{2+}-binding is responsible for substantial modifications in protein conformation affording secondary structure changes and promoting aggregation. Thermal unfolding experiments indicated that Cu^{2+} and Zn^{2+} have the ability to destabilize the protein (apo-no aggregation, Cu^{2+}-T_{agg}=68°C, Zn^{2+}-T_{agg}=65°C) leading to a total loss of secondary structure and protein aggregation. Ca^{2+}-binding does not have a large effect on S100B conformation and stability, yielding a mixture of α-helix and β-sheet secondary structure after denaturation, without forming aggregates. The study of Cu^{2+} and Zn^{2+} binding competition revealed that Cu^{2+} has the ability to displace Zn^{2+} from the binding site, with a destabilizing effect ($\Delta T_{agg} = 35$°C). However, for S100B ΔCys, although Cu^{2+} also displaces Zn^{2+}, it has the opposite effect stabilizing the protein ($\Delta T_{agg} = -5$°C). We observed that Cu^{2+}, but not Zn^{2+} or Ca^{2+}, has the ability to promote intermolecular disulfide bond formation between S100B subunits.

We hypothesize that metal induced conformational changes may account for the buildup of conformers that have increased oligomerization propensity and that this may play a role in S100B function and on its interactors. This possibility is particularly relevant considering the interplay of S100B with the Amyloid-β peptide and with Receptor for Advanced Glycation EndProducts, which are, all together, suggestive of an even more interesting engagement of S100B in Alzheimer's Disease.

Keywords - S100B, protein folding, metal ions, circular dichroism, thermal stability, conformational changes

Resumo

As proteínas são macromoléculas altamente versáteis que possuem inúmeras funções na célula. No entanto, se tivermos em conta apenas a informação existente na sua cadeia polipeptídica, estas não são capazes de realizar todas as suas funções, necessitando, portanto, da ajuda de cofactores. Os iões metálicos são importantes cofactores, estando incorporados em mais de 30% das proteínas, desempenhando funções catalíticas e estruturais. As propriedades químicas e de coordenação dos iões metálicos permitem que desempenhem importantes funções ao nível da catálise enzimática, estabilização proteica e mediação da transdução de sinal. Para além disso, os metais têm a capacidade não só de promover o folding correcto de uma proteína, como de induzir alterações conformacionais nesta. De facto, existem metaloproteínas que só conseguem adquirir o fold correcto e, desta forma, possuir actividade biológica, através da ligação de cofactores metálicos. No entanto, nem sempre os efeitos dos iões metálicos são benéficos para os sistemas vivos. Estes podem ser tão essenciais como tóxicos e, por isso, as suas concentrações têm que ser altamente controladas. Porém, nem sempre esta regulação ocorre levando a que, por vezes, estes iões se liguem a locais não nativos, promovendo a agregação proteica ou mediando ciclos redox que produzem espécies reactivas de oxigénio ou de azoto. Torna-se assim relevante o estudo e a caracterização das funções destes iões metálicos enquanto modeladores da conformação e estabilidade proteica.

Neste trabalho, pretendeu-se estudar o efeito que certos iões metálicos têm na estabilidade e conformação de uma proteína, bem como a influência que a modulação por parte dos metais tem na função proteica. O sistema modelo utilizado foi a família das proteínas S100, em particular a proteína S100B. Sabe-se que a ligação de iões metálicos às proteínas S100 induz alterações conformacionais e que as mesmas estão relacionadas com

as funções celulares destas proteínas. As proteínas S100 são, na sua maioria, homo- ou heterodímeros de baixa massa molecular (10-12 kDa). São exclusivamente expressas em vertebrados e, até à data, existem 21 membros identificados. As S100 formam o maior subgrupo pertencente à superfamília das proteínas *EF-hand*. Estas proteínas ligam Ca^{2+} a um motivo estrutural denominado *EF-hand* . Como já foi referido, a ligação do Ca^{2+} induz uma alteração conformacional que expõe uma zona hidrófoba onde ocorre a ligação de outras proteínas. Algumas proteínas S100 também têm a capacidade de ligar Cu^{2+} e Zn^{2+} em locais que não os de ligação ao Ca^{2+}. Para além disso, são altamente especializadas, apresentando padrões de expressão sub-celulares e em tecidos muito específicos. Estas proteínas são componentes principais na rede de tamponização e transdução de sinal, regulando o ciclo, crescimento, diferenciação e mobilidade celulares.

A S100B é uma proteína que liga Ca^{2+}, Cu^{2+} e Zn^{2+}, sendo altamente expressa no cérebro humano, possuindo diversas funções intra e extracelulares. Esta proteína está envolvida em vários processos patológicos em que a homeostase dos metais está alterada, tais como a Doença de Alzheimer ou a Esclerose Lateral Amiotrófica, o que representa uma função proteica modificada. Embora se saiba que a ligação de iões metálicos à proteína S100B induz mudanças conformacionais, ainda permanecem por esclarecer os mecanismos subjacentes a esta modulação e a forma como eles afectam a estabilidade proteica. Neste trabalho, estudou-se exaustivamente o efeito que a ligação de iões metálicos tem no folding e na estabilidade da citocina S100B.

O ambiente fisiológico em que a proteína se acumula, por exemplo a fenda sináptica, é rico em iões metálicos. Desta forma, a interacção proteína-metal é relevante, na medida em que pode ajudar a compreender o papel fisiológico (e também patofisiológico) da S100B.

O principal transdutor das funções extracelulares é o Receptor for Advanced Glycation EndProducts (RAGE). Guenter Fritz , colaborador do laboratório de acolhimento onde este trabalho foi realizado, observou recentemente que a interacção *in vitro* da proteína S100B com o receptor RAGE é afectada por um cross-link espontâneo entre as duas proteínas, através de uma ligação persulfureto. De forma a contornar este problema produziu uma proteína mutada, a S100B ΔCys, em que os dois resíduos de cisteína (Cys84 e Cys68) foram substituídos por serinas. Esta mutação não afectou a estrutura global da proteína. No entanto, umas das hélices ficou truncada e o C-terminal destruturado. Esta proteína mutada foi também objecto de estudo neste projecto, sendo importante para se perceber o papel das cisteínas na conformação e estabilidade da

proteína na sua forma selvagem.

Os iões metálicos, tal como a proteína S100B, estão envolvidos na doença de Alzheimer (AD), nomeadamente na interacção com o péptido Aβ. De facto, estes encontram-se associados às placas de Aβ, uma característica eminente da AD. Estudos preliminares, ainda não publicados, que estão a ser realizados no laboratório de acolhimento, revelaram um efeito de cross-seed entre Aβ e a S100B. A amiloidogénese da proteína S100B ou do péptido é favorecida na presença de amilóides pré-formados da outra proteína. Desta forma, torna-se viável a possibilidade de envolvimento da proteína na agregação proteica e neurodegeneração.

O estudo da conformação e estabilidade da proteína S100B foi realizado através do uso de vários métodos biofísicos de análise de estabilidade proteica. As alterações estruturais promovidas pela acção de iões metálicos e a estabilidade térmica da proteína foram estudadas Dicroísmo Circular (CD) de UV-longíquo.

Os resultados demonstram que tanto a ligação de Cu^{2+} como a de Zn^{2+}, são responsáveis por modificações significativas na conformação proteica, originando alterações na estrutura secundária e promovendo a agregação proteica. As experiências de desnaturação térmica realizadas indicam que tanto o Cu^{2+} como o Zn^{2+} são capazes de destabilizar a proteína. De facto, no estado apo esta não apresenta qualquer tipo de agregação proteica, mesmo após desnaturação térmica, mas quando se adiciona um destes metais, Cu^{2+} ou Zn^{2+} a T_{agg}=68°C e T_{agg}=65°C, respectivamente. A destabilização induzida por estes metais leva a uma perda total da estrutura secundária e à agregação da proteína. Por outro lado, a ligação de Ca^{2+} não tem um efeito significativo na conformação e estabilidade da proteína S100B. De facto, após desnaturação térmica, os espectros de CD revelam que a proteína apresenta uma mistura de estruturas secundárias: Hélices-α e folhas-β. De referir que a proteína com Ca^{2+} ligado não apresenta formação de agregados. Os estudos de competição de ligação de metais, com ligação de Cu^{2+} e Zn^{2+}, indicam que o Cu^{2+} tem a capacidade de remover o Zn^{2+} do local de ligação, tendo um efeito destabilizador ($\Delta T_{agg} = 35$°C). No entanto, para a proteína S100B ΔCys, embora o Cu^{2+} também seja capaz de remover o Zn^{2+}, este apresenta um efeito oposto ao que se via para a proteína wt. Neste caso, observa-se um efeito estabilizador ($\Delta T_{agg} = -5$°C).

As experiências realizadas com Géis PAGE ou SDS-PAGE na presença e ausência do agente redutor TCEP, permitiram afirmar que só o Cu^{2+}, e não o Zn^{2+} nem o Ca^{2+}, possui a capacidade de promover a formação de ligações persulfureto intermoleculares

entre subunidades da proteína S100B.

Em conjunto, estes resultados permitiram-nos propor a hipótese de que as alterações conformacionais induzidas pela ligação de metais podem explicar o aumento do número de conformações que apresentam uma maior propensão para a oligomerização. Para além disto, esta ligação de iões metálicos pode desempenhar um papel na função da proteína e na sua interacção com outras moléculas. Esta possibilidade é particularmente relevante se tivermos em conta a interacção existente entre a proteína S100B, o péptido Aβ e o receptor RAGE. Estes três intervenientes no possível papel das proteínas S100 na agregação proteica no espaço sináptico sugerem, em conjunto, uma ligação ainda mais interessante entre a S100B e a AD.

Palavras-chave - S100B, folding de proteínas, iões metálicos, dicroísmo circular, estabilidade térmica, alterações conformacionais

Acknowledgments

I would like to express my sincere gratitude to the following people, that in one way or another made the work presented on this thesis possible:

To my supervisor, Cláudio M. Gomes for his enthusiasm for science that captivated me immediately and that always kept me motivated during my work. He is surely an example of the scientist that I aspire to be in the future.

To my FCUL teacher, Ana A. Coutinho. It was because of her enthusiastic classes that I became interested for this scientific area.

To my colleagues at the Protein Biochemistry Folding and Stability group, for their friendship, constant support and help in the laboratory and for an amazing work environment: Hugo Botelho,Sónia Leal, Tânia Lucas,Pedro Fernandes, Bárbara Henriques and João Rodrigues - it is a joy to be part of this group. A special thank goes to Hugo, for his patience in answering to all of my questions and for teaching me "how things in PBFS work".

To Guenter Fritz, for the collaboration on the S100 proteins and for useful discussions about my work.

To João Freire. For always being available to help me with everything. For his helpful discussions and for the models he designed for my thesis.

To my friends and family. For their patience and support during the last months. To my mom and dad. To Ruivo and Vila Viçosa family, for the precious help in everything, every single day. To Diogo, for everything that does not fit these lines...

Contents

List of Figures

List of Tables

List of Abbreviations

AD	Alzheimer's disease
ALS	Amyotrophic lateral sclerosis
ANS	1-anilino-8-naphtalene-sulfonic acid
APP	Amyloid precursor protein
Aβ	Amyloid β
CD	Circular dichroism
C$_m$	Midpoint denaturant concentrarion
Cys	Cysteine
DLS	Dynamic light scattering
DTT	Dithiothreitol
EDTA	Ethylenediaminetetraacetic acid
K$_D$	Dissociation constant
PAGE	Polyacrylamide gel electrophoresis
RAGE	Receptor for advanced glycation endproducts
SDS	Sodium dodecyl sulfate
Ser	Serine
TCEP	Tris(2-carboxyethyl)phosphine
ThT	Thioflavin T
T$_m$	Midpoint denaturation temperature
T-ramp	Temperature ramp
UV	Ultraviolet
ΔG	Gibbs free energy variation
ϵ	Extinction coefficient

Chapter 1

Introduction

1.1 Metal Ions and Protein Folding

Metal ions are important cofactors in about 30% of all proteins, having catalytical and structural roles essential to fulfill protein functions. They have unique chemistry and coordination properties, which make them indispensable for living organisms. Moreover, they have an impact in polypeptide properties influencing protein structure and stability. Therefore, it is important to understand what are the effects of metal ions in proteins and how do they influence protein strucuture and stability.

1.1.1 Metals in Biology

Metal ions are essential to life playing important roles in all classes of biological processes. In fact, it is well-known that at least thirteen metals are indispensable for the survival of plants and animals [**1, 2**]. Calcium, potassium, sodium and magnesium are the four dominant metal ions in a cell, representing 1-2% of the human body weight. These are known as bulk metals and have an important role in processes such as nerve conduction, muscle contraction and stabilization of nucleic acids. However, not all of the essential metals are so abundant as the ones mentioned above. The less abundant trace elements, which represents only 0.01% of human body weight, include transition metals and are essential nutrients to all forms of life. These transition metals are elements of the d-block: vanadium, chromium, molybdenum, manganese, iron, cobalt, nickel, copper and zinc [**1, 3–5**]. In **Figure 1.1** is represented the periodic table of the elements showing the position of metals that play important roles in biological systems [**3**].

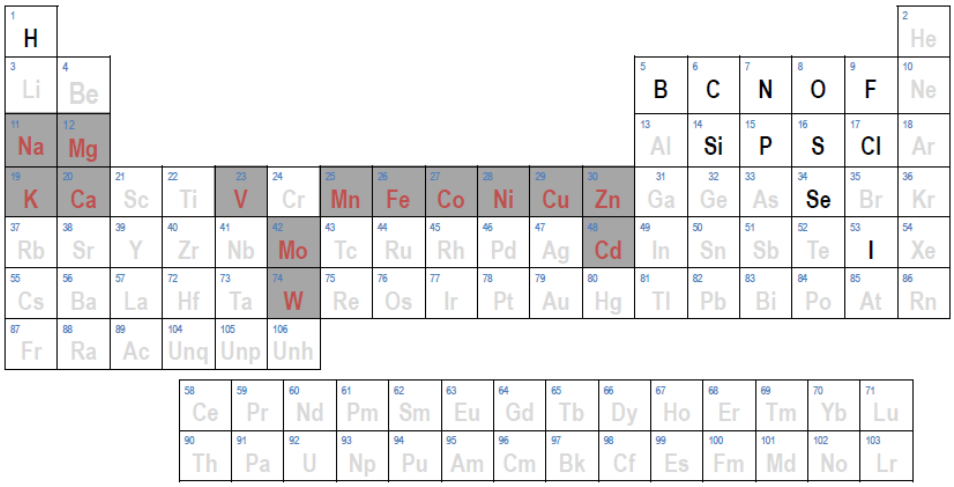

Figure 1.1: Biologically significant metals. Metal ions with biological roles are in red; the black elements have some biologically relevant function. From ref. [**6**].

Metals can be both essential and toxic. If their concentration is not regulated they could be harmful or even lethal to the organism. This toxicity appears, for example, through the formation of reactive oxygen species that have the ability to damage several cellular components including proteins, lipids and nucleic acids, which can lead to cell death.

In this way, nature has evolved with the purpose of regulate intracellular pools of metal ions, in other words, in order to maintain a balance between metal ions as essential elements and their potential toxic effect [**1, 7**].

Metal ions, in particular trace metals, have unique chemical and physical properties which make them an integral and indispensable part of more than thirty percent of all known proteins [**1, 5**]. In fact, they provide essential biochemical activities and are structurally vital to several proteins [**5**]. Recent studies indicate that 47% of enzymes require metals and that 41% contain metals in their catalytic center [**2, 8**] (**Figure 1.2**). Although metal ions are natural constituents of proteins, they could also be found as components of prosthetic groups, cofactors and several complexes before being inserted into proteins [**5**].

The metal-binding proteins can be classified into several groups according to their functions. They could act as enzymes or be electron carriers, being involved in metal or oxygen management. Iron an copper are redox-active metals and participate in electron transfer when they are bonded to metalloproteins such as cytochromes, iron-sulfur proteins and blue-copper proteins, for example. Iron and copper are also involved in oxygen

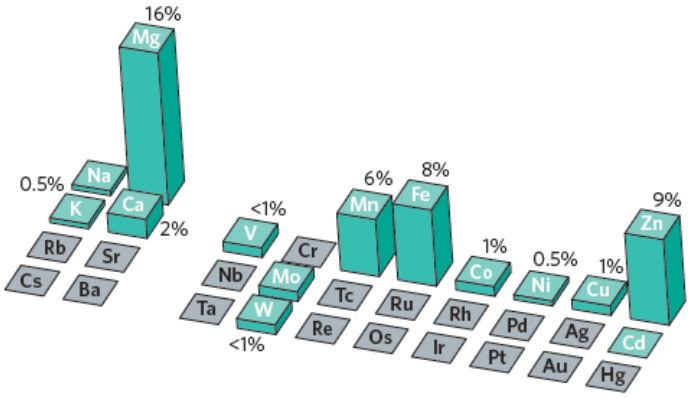

Figure 1.2: Metal ions involved in enzyme catalysis. The elements used as cofactors by enzymes are shown in blue. The height of each column represents the proportion of all enzymes with known structures using the respective metal. A single enzyme uses cadmium. The elements in grey have no biological role. From ref. [**8**].

management (storage and carriage) via metalloproteins like myoglobin, hemoglobin or hemocyanin. Enzymes like hydroxylases use magnesium, copper and zinc as cofactors. Therefore, metals are involved in several biological processes spanning from protein stabilization to enzyme catalysis and a wide variety of specific tasks essential to life processes [**1**]. They are involved in signal transduction acting as molecular ”switches”, in nitrogen fixation, respiration and photosynthesis, function as redox centers and transporting oxygen [**9**].

1.1.2 The Protein Folding Problem

Proteins are the most abundant and versatile macromolecules of the cell [**10**]. They play a key role in a wide diversity of processes such as catalysis, signal transduction, ligand binding and molecular interactions. In order to fulfill their biological activity, proteins have to acquire their native three-dimensional strucuture. This structure is attained through a process called protein folding. Protein folding is thus the physical process by which a polypeptide folds into its characteristic and functional three-dimensional structure [**11**].

This process has been under study for many years but it is not yet completely understood. It is known, since pioneer Anfinsen's work on ribonuclease [**11**] in the 1970's, that proteins can fold spontaneously without the intervention of additional entities. This means that all information that is required to specify the three-dimensional structure of

a protein is encoded solely in its primary structure. It was since Anfinsen's experiments that the thermodynamic hypothesis was born: this hypothesis postulates that if the native structure of a protein is achieved spontaneously it should correspond to the most stable conformation in a thermodynamic point of view [**11**].

Simultaneously, Levinthal focused on the kinetics and dynamics of the folding process [**12**]. In his point of view, it did not make sense that the folding mechanism would be a completely random sampling process resulting from the iteration of all possible conformations since the conformational space to be explored would be too large. If this would happen, a protein with 100 aminoacids would take 10^{29} years to fold, even assuming that sampling of each conformation would be as fast as the time required for a single molecule vibration (10^{-13} seg). This however, is inconsistent with the short time scale (miliseconds to seconds) that a protein takes to fold [**12**]. This is known as the Levinthal Paradox. According to this kinetic hypothesis, the folding of a polypeptide occurs because there are energy barriers that force proteins to follow through specific folding pathways, in which may occur intermediate states and at the end of which is the native state. Nowadays, the majority of authors accept the theoretical formulation of the energetic funnel to illustrate the mechanism of protein folding (**Figure 1.3**). According to this point of view, there is no single pathway, but several possible ways of folding to be followed in parallel by all the denatured polypeptide chains until they reach their native state. The folding process can present multiple intermediates and the energy landscape correspondent can display kinetic traps with high energy barriers. The external border of the energy landscape is populated by the high energy denatured states that can flow through the funnel by alternative pathways until they reach, the native conformation [**13**].

It should be noted that the native state and the folded state of a protein are not synonyms. The folded state of a protein is a compact three-dimensional structure floating around a limited number of conformations. It implies secondary structure and several weak interactions that have the ability to stabilize this compact state. On the other hand, the native state is not necessarily correspondent to the folded state. In fact, it corresponds to the biological active conformation but, for example, it can be a disorganized state, without defined secondary structure. Usually, in these cases, the native state acquire a defined structure when it is performing its biological function.

The unfolded state of a protein is an unstructured state without defined secondary, tertiary or quaternary structure elements. This state can be induced *in vitro* by us-

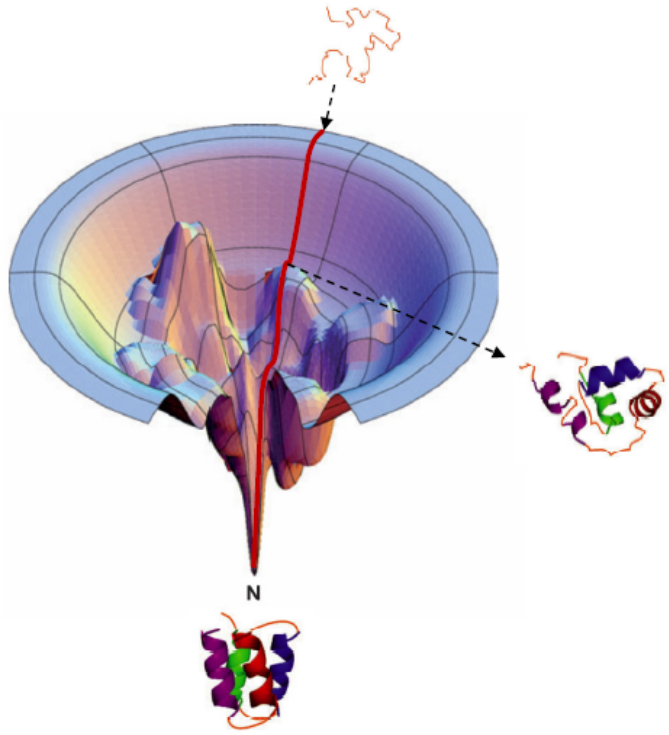

Figure 1.3: Three-dimensional representation of the folding funnel. From ref. [**14**].

ing drastic conditions like high urea or guanidinium concentrations, high temperatures, drastic pH values etc. The unfolded state can be seen as a mixture of several states that can be interconverted.

Except for some special cases, the folded state is the most stable one. There are two possible explanations for this stability: the thermodynamic and the kinetic hypothesis [**15**].

In the thermodynamic hypothesis there are several factors contributing to the variation of free energy in protein folding **Figure 1.4**. Some favor the folded state (internal interactions and hydrophobic effect) and other favor the unfolded state (conformational entropy) [**17**]. Conformational entropy concerns the global entropy of the polypeptide chain and, because the folded state is much more organized than the unfolded one, this entropic factor favors the unfolded state. However, the entropic component is counter balanced by the hydrophobic effect, which favours internal organization and thus the folded state. The origin of this entropic factor is on the unfavorable restrictions imposed by the hydrophobic amino acids exposed to solvent. Finally, there is an enthalpic factor

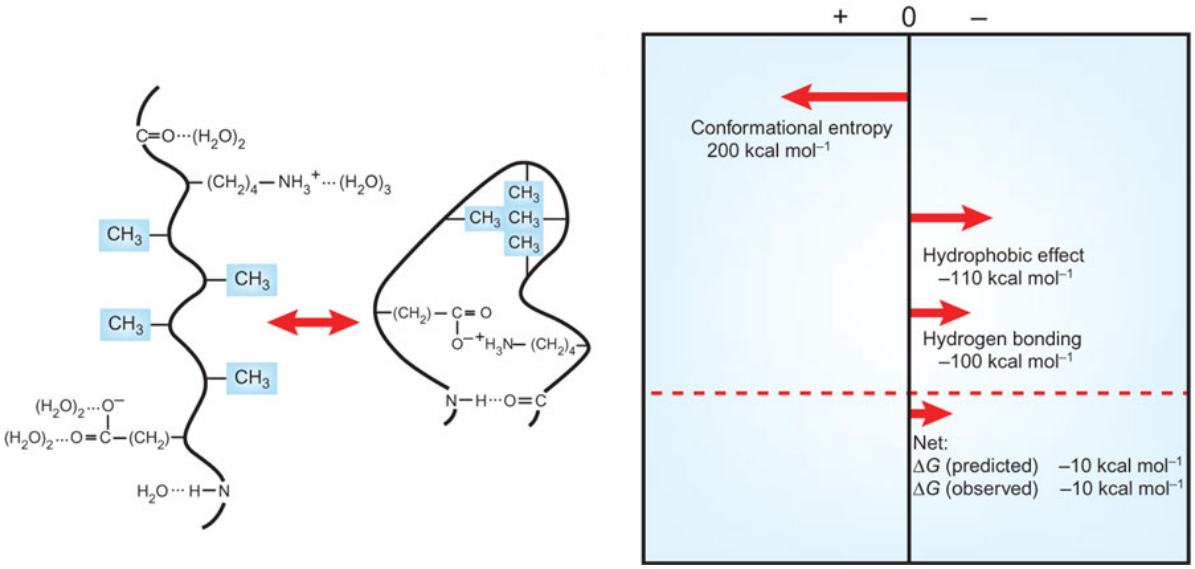

Figure 1.4: Stabilizing and destabilizing forces on the folding of a protein. From ref. [**16**].

favoring the folded state which is the result of the sum of the internal covalent and noncovalent interactions that stabilize the folded state: disulfide bridges, charge-charge interactions, hydrogen bonding and van der Waals interactions [**18**]. The thermodynamic hypothesis states that the folded state is thermodynamically more stable than the unfolded one [**19**]. Moreover, it was already experimentally showed that the free energy difference between the two states is small.

There is another possible explanation for protein stability which is the kinetic stability hypothesis [**15**]. This hypothesis states that in case the unfolded state is thermodynamically more stable than the folded one, there is a high energy barrier separating the two states trapping proteins in the folded conformation.

Although protein folding is a fundamental process and the function of proteins depends on it, sometimes this process does not occurs as expected. In fact, in the cellular environment, a fraction of all synthesized proteins fail to fold into the native structure [**20**]. In order to deal with the challenges of the process of folding, biological systems developed a specific protein machinery - the protein quality control (PQC) system - that assists the folding process with no effect in the selection of the native structure and in the degradation of incorrectly folded conformations. The PQC has the ability to supervise folding, disable aggregation and remove misfolded or damaged polypeptide chains before they exert toxic effects [**21**]. The system is composed by molecular chaper-

ones, specialized intracellular proteases and accessory factors that regulate the activity of chaperones and proteases or provide communication between the various components [**21**]. However, the PQC systems sometimes fails and when this takes place brings severe biological consequences that result for example in the so-called misfolding diseases [**22**] or protein deposition in the form of insoluble amyloid fibrils. These amyloid fibrils are characteristic of neurodegenerative disorders such as Alzheimer, Parkinson or prion diseases [**23–25**].

Some proteins are only able to acquire its native structure in the presence of cofactors such as metal ions. In fact, metal ions are key factors in the folding of several metalloproteins.

1.1.3 Metal Ions in Protein Folding

Around 30% of human proteins contains a metal ion as a cofactor. In fact, metal ions play an important role in protein folding and stability and despite the huge amount of available information about the structure of several metalloproteins, this role is complex and remains mostly unknown. In order to understand this relationship we need to address how metals bind to proteins: before, during or after protein folding. It is also important to understand how a protein selects a specific metal from the pool of metal ions that are present in the cellular environment.

There are several possible scenarios that can be outlined for the folding of metalloproteins (**Figure 1.5**). The metal insertion into different metalloproteins is likely to occur at different moments of the protein biogenesis process. Metal ions may bind to a protein during translation, i.e, as the polypeptide chain emerges from the ribosome, after polypeptide release but before it is completely folded or after polypetide acquire its folded conformation.

Metals may induce protein folding or protein conformational changes. Proteins emerge from the ribosome in the unfolded or partially folded state and metal insertion may be necessary for folding. Some newly synthesized apo proteins (metal-free) are not able to acquire its folded state until metal insertion. Zinc finger domains are an example of this since they can only fold to the native structure in the presence of zinc. There are some cases in which metal ions bind to the nascent polypeptide chain as it emerges from the ribosome. For example, we can enumerate iron, from heme, that binds to unfolded state of cytochrome b_{562} and copper, which remains bounded to azurin even

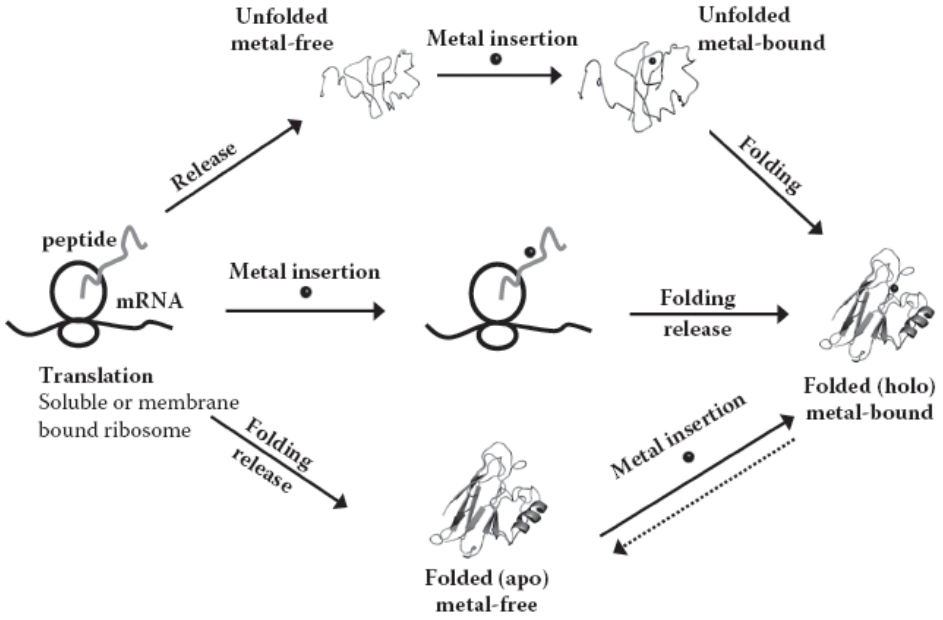

Figure 1.5: Distinct pathways for metalloproteins folding. Metal insertion into different metalloproteins is likely to occur at different steps of protein biogenesis process. From ref. [**1**].

after unfolding of the protein. Some metalloproteins, like most calcium-binding proteins (e.g. S100 proteins), are able to acquire its folded structure without metal binding. In these cases metal incorporation is necessary for conformational changes or to fulfill catalytical functions. These calcium binding proteins remain in the folded state even if metal is released from the holo (metal-bound) state. However, for other proteins, metal release can result in either misfolding or unfolding as a result of conformational destabilization [**1**].

The next sections briefly describe the interplay between metal ions and protein folding, focusing in the most relevant metal ions — iron, zinc, copper and calcium.

Iron

Iron is the transition metal most abundant in the human body. It has oxidation states ranging from -2 to $+6$ but the two most biologically relevant are Fe^{2+} and Fe^{3+} [**5**]. These two stable oxidation states make iron a very versatile element which renders this metal an important redox mediator. In proteins, it is found in an unparalleled variety of sites and cofactors, including, for instance, Fe-O-Fe sites, heme groups and iron-sulfur clusters [**26**]. Incorporation of iron into proteins may take place in three different ways:

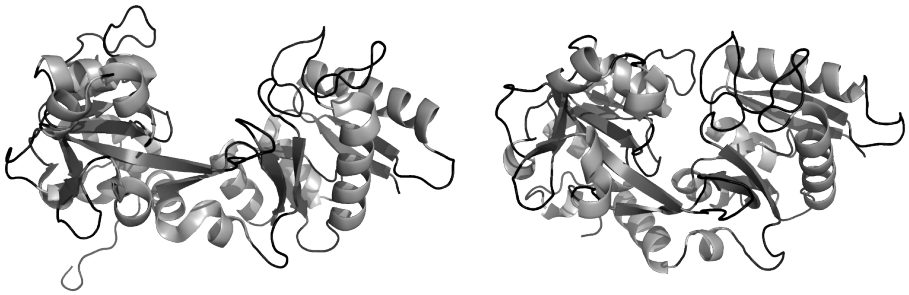

Figure 1.6: Fe^{3+}-induced conformational changes in human transferrin. The apo form (1BP5, left) has an open conformation. When Fe^{3+} binds, the holo protein (1A8F, right) adopts a different conformation. The two protein domains close around the inter-domain hinge enclosing the metal ion in the protein core[**6**]. Image rendered using PyMOL software [**27**].

in the form of a heme prosthetic group, in iron sulfur clusters or by the bound of iron into non-heme iron proteins.

Iron has an important role in iron-proteins folding. One of the best studied cases resulting from this interplay is the folding of cytochrome c. In this protein the iron is inserted in a heme group which is covalently bound to the polypetide. It has been shown that the substitution of the metal ion (Fe^{3+}) in the heme group is associated with important consequences in the protein folding [**28**–**30**]. Moreover, the removal of the heme group leads to secondary and tertiary structure loss [**31**]. Although this suggests that heme is necessary for cytochrome folding there are other evidences that may suggest otherwise. It was observed a spontaneous folding of apo cytochrome c_{555} from *aquifex aeolicus* [**32**]. Furthermore, apo cytochrome c_{551} from *Pseudomonas aeruginosa* unfolds reversibly and acquires a compact marginally stable conformation [**33**]. Another example is transferrin that undergoes conformational changes after iron binding, which stabilizes the protein and alters the unfolding pathway of it [**34**] (**Figure 1.6**).

Zinc

Zinc is essential to all forms of life and is the second most abundant transition metal in several organisms, including humans [**35**]. This metal is also the second most abundant metal ion in enzymes participating in at least 300 enzymatic reactions [**2, 36**]. Zinc is a redox inert metal ion which make it a generally considered less toxic than redox active metals such as iron and copper [**5**].

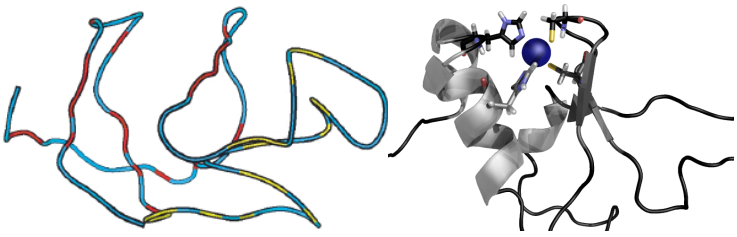

Figure 1.7: Folding of a zinc finger domain. Structure of a zinc finger domain (2CT5, right). This domain only acquires the secondary structure upon zinc binding. In the absence of zinc the domain is completely unstructured (left).

As mentioned before, zinc is an important cofactor in catalysis since it has a rapid ligand exchange rate that allows an efficient turnover of reaction products [**37**]. Although zinc is a redox inactive-metal ion it is necessary to maintain the proper structure and function of several proteins [**36**]. Incorporation of zinc in a variety of biological systems is due to its structural and thermodynamic properties and also with the abundant bioavailability of this metal.

The folding of several proteins is dependent of zinc ions, in particular proteins containing zinc finger domains. Zinc fingers are the most abundant structural domain in the human proteome (present in 3% of all proteins) and they are also the most prevalent zinc binding motif [**38, 39**]. The classic structure of zinc finger domains has a $\beta\beta\alpha$ fold where zinc ion binds. The topology of the domain is kept in place by zinc ion, which is strictly required as an essential structural determinant (**Figure 1.7**). In fact, if the coordinating residues are removed, the fold is disrupted [**1**]. Moreover, the apo form of zinc finger domains is unstructured and acquires only the proper fold upon zinc binding. Furthermore, the zinc-bound domain is stabilized and becomes competent in DNA binding [**40**].

Other proteins like Cu, Zn-superoxide dismutase (Cu, Zn-SOD1) require zinc as cofactor. Although zinc does not take part of the catalysis it is crucial for the protein folding and thermostability [**41**].

Yeast alcohol dehydrogenase requires two zinc ions per subunit, one sits in the catalytic site and the other has a structural role. In this case it has been described that zinc is essential for protein proper folding, confering a higher chemical stability and a higher folding cooperativity [**42**–**44**].

Copper

Copper is a crucial transition metal in biology as it plays a key role in all living organisms, being essential to many forms of life. In biological systems it can be found predominantly in two oxidation states Cu^{1+} and Cu^{2+}. Cu^{2+} is the most effective bioavailable divalent cation for binding organic molecules as is Cu^{1+} for monovalent cations, due to electron affinity. It has an important role in cellular redox reactions, being indispensable for the catalysis and structure of a wide range of enzymes whose activities are essential for several and important biochemical and regulatory processes [**5**].

Like other metal ions copper is necessary for the proper fold of some proteins. It is a cofactor for proteins involved in electron tranfer, oxidase and oxygenase activities, acting as a biological activity centre for proteins like Cu, Zn-SOD, ceruloplasmin, cytochrome c oxidase, tyrosinase and dopamine β-hydroxylase [**45**].

Pseudomonas aeruginosa azurin is a blue-copper protein that contains a single copper ion. The apo and the holo form of this protein have a three-dimensional structure identical. However, this metal ion have a significant effect in azurin's thermodynamic stability. In fact, it was reported that copper oxidized is more thermodinamically stable than the reduced copper form. Moreover, the holo form is more stable than apo-azurin [**46**]. The stability of apo protein is 6.9 kcal.mol^{-1} but after the binding of Cu^{2+} it raises to 12.4 kcal.mol^{-1}. It was proposed that the mechanism by which copper increases azurin thermodynamic stability is based only on slower unfolding, as it was observed that holo-azurin unfolds much slower than apo-azurin. The metal ion binds the native and the unfolded state of azurin which is important for folding kinetics. If Cu^{2+} binds before folding it accelarates the kinetics (miliseconds) relatively to copper binding after apo protein folding is complete (minutes to hours) [**47**] (**Figure 1.8**).

Copper is also required for the stability of ceruloplasmin. This protein binds six copper ions and like azurin, holo protein is more stable than apo-ceruloplasmin (Tm increases from 15 to 25°C) [**48**].

Calcium

Calcium is an ubiquitous second messenger that can transduce extracellular signals into several intracellular responses. Thereby it can regulate many biological processes such as muscle contraction, neurotransmitter release, fertilization and cell growth [**49**]. Diverse enzymes activities are also controled by calcium ions [**50**]. Due to its pivotal role, the

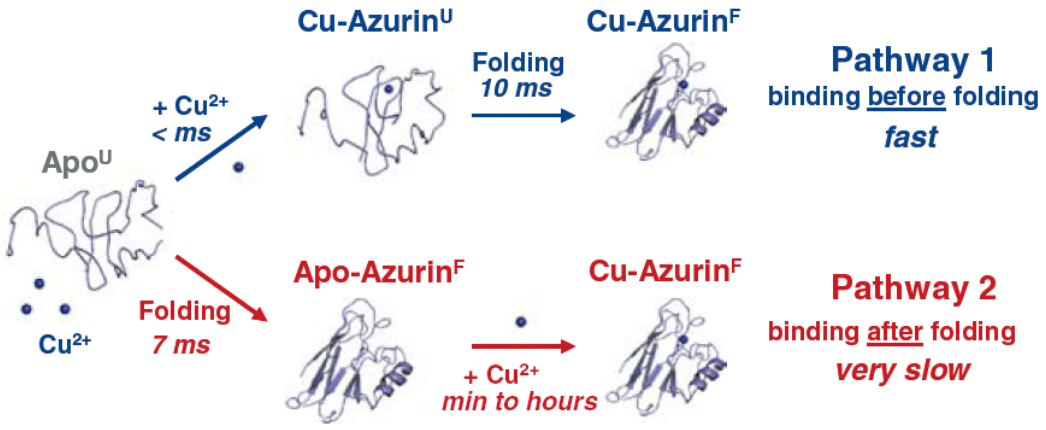

Figure 1.8: Formation of active Cu-Azurin. Cu^{2+}binding to Azurin before or after folding is an important factor in folding kinetics of this protein. From ref. [**47**].

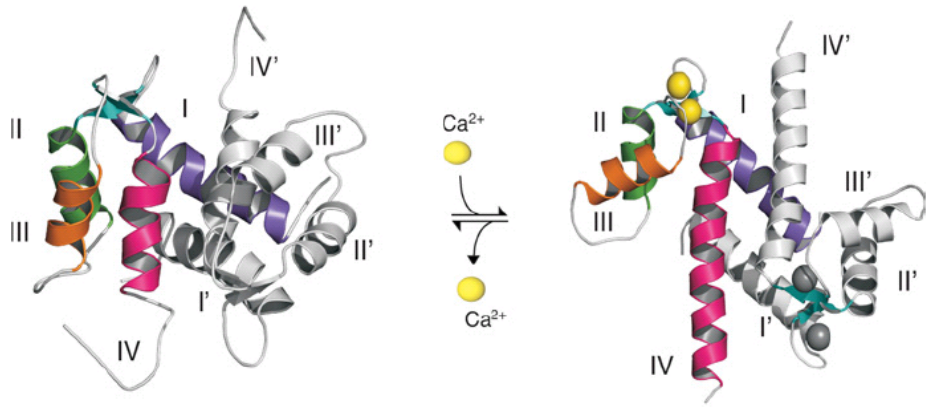

Figure 1.9: Calcium-dependent conformational change in S100 proteins. Three-dimensional structures of Apo S100A11 (left) and Ca^{2+}-bound S100A11(right). As could be seen in the figure, Ca^{2+}-binding induces a conformational change in the structure of S100A11. From ref. [**49**].

cellular machinery maintain tigh control of this ion concentration,which ranges from resting levels near 100 nM to signalling levels near 1 μM [**49**]. Calcium ions control a wide variety of cellular events in part via interaction with a large number of Ca^{2+} binding proteins [**50**].

The most abundant calcium binding motif is the helix-loop-helix EF-hand, present in several proteins, including S100 proteins, calmodulin and troponin C. Some EF-hand proteins undergo a substantial conformational change upon Ca^{2+} binding that results from the lateral motions of the two helices that flank the Ca^{2+} binding residues[**1**].

This conformational change exposes a hydrophobic surface necessary for protein-protein interactions (**Figure 1.9**).

Calmodulin, a well studied EF-hand protein, regulates enzyme activities, neurotransmiter release, cell proliferation and DNA repair. The majority of these activities require interaction with other proteins which is dependent of calcium binding [**6**].

Calcium has an important role in the folding of parvalbumin. The apo-parvalbumin has been described as natively disordered [**51**]. In the calcium-bound state the protein rests in a compact globular state, with the EF-hand in an open state. However, after metal ion release occurs a fast (∼60 ps) conformational rearragement that leads to a decrease in helical content (>20%) and to an enhanced residue solvent accessibility [**52**].

Another example of calcium-dependent conformational changes in EF-hand proteins relies on bovine α-lactalbumin. This protein is able to regulate lactose synthesis in a calcium-binding dependent manner. Calcium increases its folding rate by three orders of magnitude [**53**–**55**] and couples refolding to the generation of the native disulfide bridge [**56**]. All together these facts suggest that occurs a calcium regulation of lactose synthesis through the control of protein folding. Moreover, it is known that calcium accelerates the folding of α-lactalbumin by decreasing the energy barrier between the molten globule and the transition state [**55**].

1.2 S100 Proteins

Metal ion binding to S100 proteins are associated with conformational readjustments that underlie the cellular functions of these proteins. In this project the protein model system used was S100 protein family, in particular the S100B protein.

1.2.1 The Family of S100 Proteins

The name of the S100 protein family is due to the fact that the first identified S100s were obtained from the soluble(S) bovine brain fraction upon fractionation with 100% saturated solution of ammonium sulfate [**57**].

This protein family represents the largest subgroup within the superfamily of EF-hand Ca^{2+} binding proteins [**3, 49, 58**]. The family of EF-hand proteins can be divided into two primary classes: Ca^{2+} sensors, which transduce the Ca^{2+} signals, and Ca^{2+}

signal modulators, which are involved in uptake, transport and buffering of the Ca^{2+} signal. The majority of the members of the S100 protein family are Ca^{2+} sensors. Only S100G acts as a Ca^{2+} buffer sequestering Ca^{2+} in the cytoplasm after a raise in metal concentration [**59**].

S100 proteins are exclusively expressed in vertebrates. This family comprisis 21 members identified up to date in humans. Furthermore similar numbers are found in other mammalia based on genomic analysis. Other diverse branches of S100 proteins were found in other vertebrates [**58**].

Each member of S100 protein family is encoded by a separate gene which are mostly clustered in region 1q21 of human chromosome 1 [**60, 61**]. The human S100 proteins have a gene structure highly conserved, in general comprising three exons and two introns [**59**]. This region contains the genes from S100A1 to S100A16. The genes of other members of the family like S100B, S100P or S100Z are found, respectively, in chromosomes 21, 4 and 5 [**58**]. It should be noted that the level of sequence identity among these proteins within one species varies. For human proteins the identity ranges between 22% and 57% [**62**].

S100 proteins have cell- and tissue-specific expression patterns as well as specific subcellular localization, pointing towards a high degree of specialization [**3, 58**]. This level of specialization has meant that the S100 proteins are involved in several cellular processes such as cell cycle regulation, growth, differentiation and motility [**59**]. Due to these multitude of functions it is quite normal to find that these proteins are implicated in several human diseases, like different types of cancer, with altered expression levels of S100 proteins, inflammatory and autoimmune diseases [**63**] and neurodegenerative disorders, such as Alzheimer's Disease (AD) [**64**].

Metal ions have the ability to modulate the conformational properties and functions of S100 proteins. As mentioned in section 1.1.3 the binding of Ca^{2+} to proteins with EF-hand domains triggers conformational changes that are necessary to the interaction with other proteins (see section 1.3.3). In the case of S100G, the Ca^{2+}-induced conformational change is small and does not lead to the exposure of a hydrophobic patch [**59**].

Zn^{2+} binding have also a role in folding and function of many S100 proteins. Furthermore, the Receptor for Advanced Glycation Endproducts (RAGE) has been identified as a new target for several S100 proteins. Several reports showed that an increasing number of S100 proteins are bonded extracellularly to RAGE [**65–68**] or to Toll-like

receptor 4 [**69**].

1.2.2 Structural properties

S100 protein family members are acidic proteins with a molecular mass that ranges between 10-12 kDa. These proteins have the ability to form homodimers, heterodimers and even oligomers but with largely different preferences. This fact, in particular the formation of heterodimers, may contribute to S100 functional diversification [**59**]. Almost all S100 proteins exist as dimers at physiological conditions. The exception is S100G, which exists as a monomer. However, in a general way, these dimers are linked non covalently and, therefore, it is observed a monomer-dimer equilibrium. This equilibrium is strongly dependent on the ionic strength of the solution. It has been reported that at higher ionic strengths S100B protein, for example, exists predominantly as a homodimer. In contrast, lowering the ionic strength results in a higher formation of monomeric protein [**70**]. It was also shown that other S100 proteins might exist as monomers at very low protein concentration in the cell. The physiological function of these monomers is not known yet. It was proposed that the equilibrium between monomers and homodimers might facilitate the formation of heterodimers in the cell. The list of known S100 heterodimers is becoming larger. Until now it is known that S100B protein forms heterodimers with S100A1, S100A6 and S100A11; S100A1 with S100A4 and S100P; and S100A7 with S100A10. Moreover, non-covalent multimers were observed for S100A12, S100A8/A9, S100B, S100A4. It was also observed a Zn^{2+}-dependent tetramer for S100A12. The formation of S100A8/A9 heterodimers is more favorable than the formation of S100A8 and S100A9 homodimers. In fact, if we compared the structure of the heterodimer with the structure of the corresponding homodimers we can observe that the solvent exposed area is reduced in the heterodimer, which can be the driving force for its formation [**58**].

EF-hand Ca^{2+}-binding

The name EF-hand was first used by Kretesinger and Nockolds in 1973 and is a graphical description of the calcium-binding motif observed in parvalbumin [**71**].

This structural motif became very widespread, found in a large number of protein families [**74**]. In fact, the EF-hand motif is one of the most common in animal cells [**75**]. S100 proteins belong to the Ca^{2+}-binding EF-hand motif superfamily [**63**]. These proteins present some variation in their sequence but despite that, their tridimensional structure exhibit highly conserved key structural features and common to all members of the

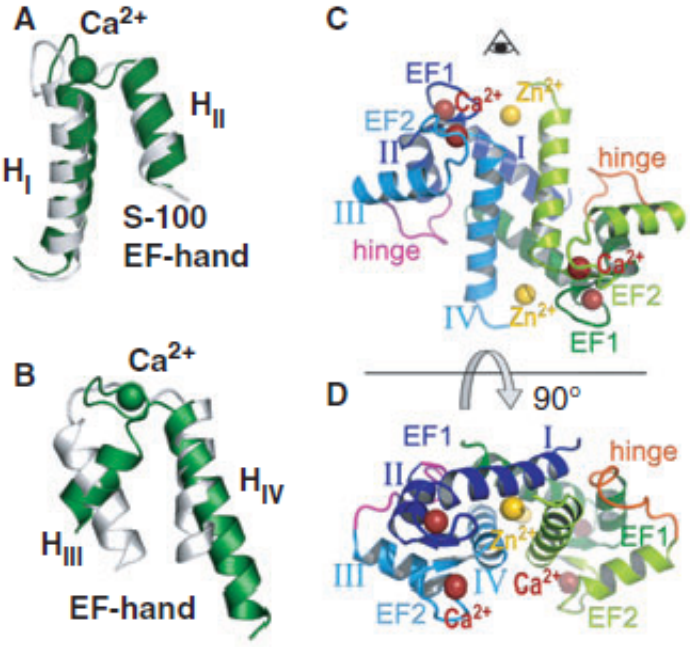

Figure 1.10: Structure of S100 proteins. (A-B) Ca^{2+}-driven conformational changes at the EF-hand in S100 proteins. Structure of the N-terminal, S100-specific EF-hand (A) and the C-terminal, canonical EF-hand (B) in the metalfree (white) and Ca^{2+}-bound (green) form of S100A6. (C-D) Structure of the human S100B homodimer loaded with Ca^{2+} and Zn^{2+} [**72**]. (C) Side view; (D) Top view.

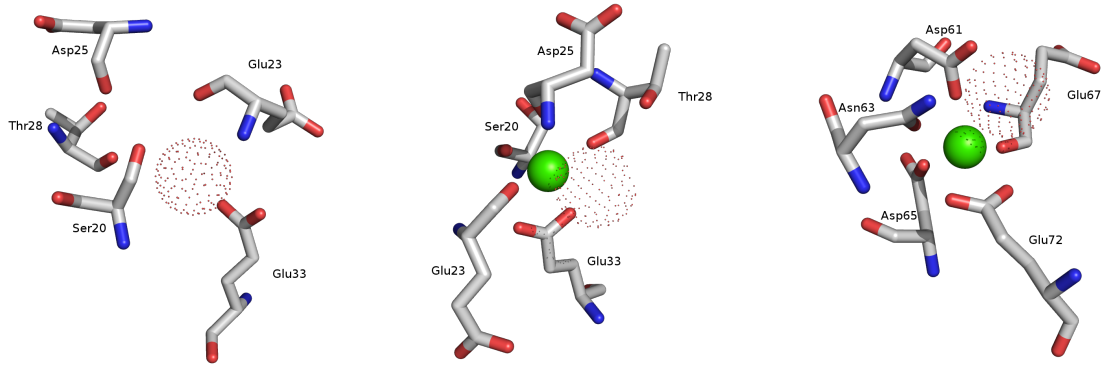

(a) a **(b)** b **(c)** c

Figure 1.11: Ca^{2+} binding sites of S100A6 protein. a) Ca^{2+}-free S100-specific EF-hand **b)** Ca^{2+}-loaded S100-specific EF-hand **c)** Ca^{2+}-loaded canonical EF-hand. Image rendered using PyMOL software [**27**] (PDB codes 1K8U, 1K96)[**73**].

family. Each S100 monomer is composed by two EF-hand helix-loop-helix structural motifs arranged in a back-to-back manner and connected by a flexible linker (**Figure 1.10**B). The C-terminal EF-hand contains the classical Ca^{2+}-binding motif, common to all EF-hand proteins. The Ca^{2+}-binding loop has a typical sequence signature of 12 aminoacids and is flanked by two helices: H_{III} and H_{IV}. Ca^{2+} is coordinated mainly by amino acid side chains. The N-terminal EF-hand has a different architecture distict from the canonical EF-hand motif. Here, Ca^{2+} is mainly coordinated by backbone carbonyls. It contains 14 specific aminoacids motif, a consensus-sequence motif, flanked by helix H_I and H_{II} (**Figure 1.10**A). As this motif is characteristic of S100 proteins it is called the 'S100-specific' or 'pseudo EF-hand'. In both EF-hands Ca^{2+} is coordinated in a pentagonal bipyramidal geometry. There are six residues involved in the binding: X, Y, Z, -X, -Y, and -Z [**59, 76**] (**Figure 1.11**). All of them are ligands except the residue -X that is occupied by a water molecule. At position -Z there are a glutamate or an aspartate residue which makes possible the binding to Ca^{2+} in a bidentate coordination manner, since it provides a carboxylate group for the binding to the metal ion. The interface of S100 homodimer is formed by helix H_I of the N-terminal and helix H_{IV} of the C-terminal, from both monomers (**Figure 1.10**C-D). The helices build a compact and stable four helix bundle [**59**]. S100 proteins bind usually four Ca^{2+} ions per dimer with a K_d=20-500 μM and with strong positive cooperativity [**77**].

Zn^{2+}-binding sites

Unlike other EF-hand proteins, many S100 proteins have the ability to bind Zn^{2+} with high affinity (K_d=4 nM to 2 mM) [**78**]. This occur in binding sites distinct from the EF-hand Ca^{2+}-binding sites. Moreover, in some cases, it has been proposed that Zn^{2+} instead of Ca^{2+} regulates the biological function [**59**]. In fact, it has been reported that the interaction between S100B and tau protein is Ca^{2+}-independent but Zn^{2+}-dependent [**59**]. However, most of the reported Zn^{2+} constants are in the μM range, which stands in contrast with the low nM concentrations of free Zn^{2+} (2 to 10 nM) in cytoplasm. Due to this low concentration, the binding of Zn^{2+} to the majority of S100 proteins does not occur in the cytoplasm, being S100B and S100A6 two examples [**59**]. Zn^{2+}-binding might occur in vesicles that contain a higher concentration of this metal (μM to mM), or in the extracellular space, which has Zn^{2+} concentrations in the μM range [**59**].

S100 proteins have the ability to bind Zn^{2+} in two different ways and because of that they can be divided into two groups. The first one involves Cys residues in Zn^{2+} coordination

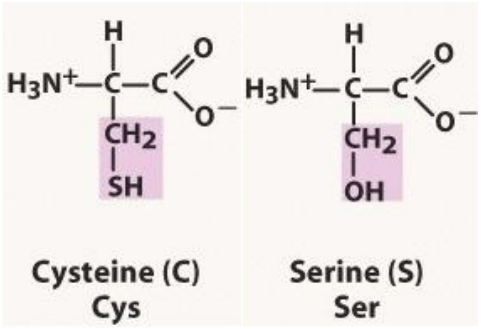

Figure 1.12: Structural difference between a Cys and a Ser residue.

and the second group binds Zn^{2+} exclusively via the side-chains of His, Glu and Asp residues [**58**]. An example of the first group is S100A2, in which Zn^{2+} is coordinated by residues from different monomers [**79**]. S100A7, S100A8/A9, S100A12 and S100B are members of the second group and it is available detailed structural information, mainly by X-ray, about them. S100A7, S100A12 and S100B can bind two Zn^{2+} ions per homodimer at dimer interface. The dimer is additionally stabilized because the Zn^{2+} ions are coordinated by residues from both subunits [**80**–**82**].

Cu^{2+}-binding sites

A number of S100 proteins also bind Cu^{2+}. This is the case of S100A5 [**83**], S100A12 [**84**], S100A13 [**85**] and S100B [**86**]. The binding of copper frequently occurs at the same sites to which Zn^{2+} binds but with different affinities (K_d=0.46-55 μM) [**83, 86, 87**]. S100B, one of the most abundant protein in the human brain, also binds Cu^{2+}. It has been sugested that Cu^{2+}-binding to this protein might have a putative neuroprotective role. Bovine S100B can efficiently sequester copper ions and hereby supress copper-ion-induced cell damage [**59, 86**].

1.3 S100B Cytokine

S100B, a 10.7 kDa protein, is a member of S100 protein family. It was originally discovered in glial cells, being the first described protein of the family [**57**]. It is highly expressed in astrocytes and is one of the most abundant soluble proteins in human brain, constituting 0.5% of them [**72**]. S100B functions as both an intracellular Ca^{2+} receptor and an extracellular neuropeptide [**88**–**90**]. The binding of Ca^{2+} to S100B protein have important functional implications. The main transducer of extracellular functions of

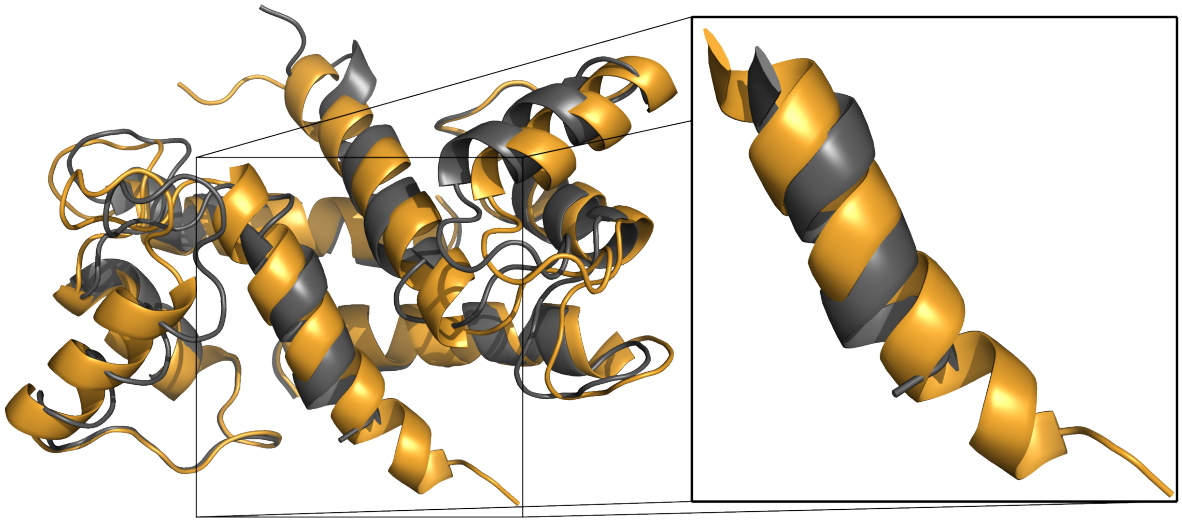

Figure 1.13: Structural alignment of S100B wt and S100B ΔCys. S100B wt and S100B ΔCys are represented in orange and grey, respectively. Image rendered using PyMOL software [**27**].

this protein is RAGE (section 1.3.3). In vitro, S100B-RAGE interaction is affected by the spontaneous cross-link between the two proteins through a disulfide bond. In order to circumvent this problem, Fritz et al produced a S100B ΔCys protein. This protein is a Cys to Serine(Ser) mutant of S100B wt protein. The two mutated residues of S100B ΔCys, Cys68 and Cys84, are near C-terminal. This is an appropriate replacement since the diference between Cys and Ser is only in one atom (**Figure 1.12**).

The mutation does not affect the overall structure of the protein. However, as we can see in S100B wt and S100B ΔCys structural alignment (**Figure 1.13**) the helix H_{IV}, where Zn^{2+} binds is truncated and the C-terminal is unstructured. After co-crystallization trials it was observed that the C-terminal where Cys84 is located got disordered upon mutation to Ser. Usually the C-terminal becomes even more ordered upon Ca^{2+} binding, which not occur with the mutant. Moreover, several Phenylalanine residues in the C-terminal are required for target binding which are disordered in the mutant protein.

The data related to S100B ΔCys protein were supplied by Fritz and Betz (unpublished observations in the scope of an ongoing collaboration with our Protein Biochemistry Folding and Stability group - http://www.uniklinik-freiburg.de/neuropathologie/live/forschung/ag-g-fritz.html?raw=true).

1.3.1 Structure and Metal Binding Properties

S100B protein has a structure typical of S100 protein family (see section 1.2.2) (image S100B structure). The three-dimensional structures of S100B, solved by NMR and crystallography, are reported for the calcium-free state [**91, 92**], calcium bond state [**67, 93–95**], with both Ca^{2+} and Zn^{2+} bond [**96**] as well as in the presence of target protein derived peptides (p53 [**97**], Ndr-kinase [**98**], capZ [**99**]). In all of these structures, S100B is displayed as a homodimer with an affinity so high (K_D in picomolar range or lower) that under all biological circumstances the monomers are absent [**100**]. Although S100B is mainly found as a homodimer, active tetramers and hexamers have been reported [**67**].

The N-terminal EF-hand of this protein suffers only minor conformational changes upon Ca^{2+} binding. However, the C-terminal EF-hand exhibits a significant structural change that exposes hydrophobic surfaces that allows the interaction with other proteins [**59, 101**]. The change of conformation in this C-terminal domain correlates a 90° change in angle between helix H_{III} and H_{IV} upon Ca^{2+}binding [**102**].

S100B binds four calcium ions per dimer with moderate affinity (K_d 2-20 μM). In physiological ionic strength this protein binds also four Zn^{2+} ions with high affinity (K_d 0.1-1 μM). Tne Zn^{2+} sites are six to eight [**77, 103**]. The affinity of Ca^{2+} for S100B increases about 10-fold in the presence of Zn^{2+} [**103**]. Moreover, S100B also binds four copper ions per homodimer with sub-micromolar affinity (K_d =0.46 μM) [**59**]. It has been suggested that this protein plays a role against copper induced oxidative stress in cells, having a neuroprotective function [**86**]. It should be noted that zinc and copper are two metal ions highly abundant in senile plaques [**59, 101, 102, 104**].

1.3.2 Cellular functions

S100B protein, like S100 protein family, possess several intra- and extracelullar roles **Figure 1.14**. In terms of intracellular functions S100B protein interacts with cytoskeleton through the modulation of microtubule assembly in a Ca^{2+}- and pH-dependent manner. It has also an important role in cell proliferation and survival, since its levels are elevated in certain tumor cells and in astrogliosis. This protein can also inhibit cell differentiation and is involved in the regulation of several enzymes. These functions are all Ca^{2+}-dependent. Moreover, regulation of Ca^{2+} homeostasis in astrocytes is another important intracellular function of S100B protein [**105**].

S100B is secreted from glial cells to the extracellular space upon changes in intracellular

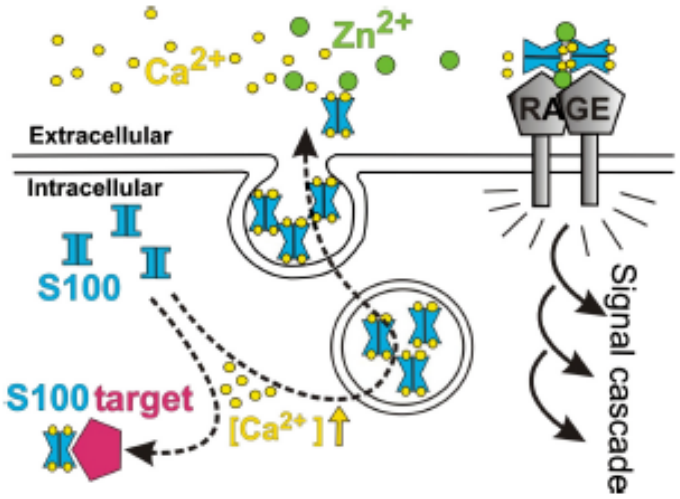

Figure 1.14: Intra- and extracellular functions of S100 proteins S100 proteins act as Ca^{2+}sensor proteins in the cell and transmit a signal by Ca^{2+}-dependent binding to a target protein, regulating its biological activity. Furthermore, several S100 proteins are secreted upon a Ca^{2+}signal. Extracellularly in the presence of high concentrations of $Ca^{2+}$and Zn^{2+}, S100 proteins can form polymers and bind to the receptor RAGE. From ref. **[62]**

Zn^{2+} and Ca^{2+} concentrations by vesicular transport. In the extracellular space it exhibits cytokine-like functions **[106]**. The extracellular action of this protein is strongly dependent on its concentration; at nM levels it exhibits a neuroprotective role, promoting neuronal survival and stimulating neurite growth but at μM concentration it promotes neuronal apoptosis, leading to the induction of pro-inflammatory cytokines and inflammatory stress-related enzymes **[104, 107–111]**. The extracellular regulatory activities of S100B have an effect on neurons, astrocytes, microglia, monocytes, macrophages, myoblasts and in other cells **[105]**.

High extracellular levels of S100B protein are associated with several neurological disorders including AD, multiple sclerosis, amyotrophic lateral sclerosis, schizophrenia, epilepsy,hypoxia and traumatic brain injury **[88–90, 112, 113]**. Extracellular S100B exerts dose dependent neurotrophic and neurotoxic action and both effects are mediated in the brain by RAGE (section 1.3.3) **[107, 114, 115]**.

1.3.3 S100B Protein Interactors

p53

p53, a tumor supressor protein, is a homotetrameric transcription factor that regulates several cellular processes. It has a crucial role in the control of cancer being responsible for preventing tumorigenic transformation in response to stress. This control is performed through the induction of cell cycle arrest or apoptosis [**116**].

Calcium binding induces a conformational change in S100B structure which destabilizes the protein quaternary structure and allows the interaction with other proteins, in particular with p53 [**116**]. There are some doubts regarding the role of S100B in p53 function. However, there are reports suggesting that this protein binds directly to the p53 tumor suppressor protein in melanoma [**117–120**], reduces p53 protein levels [**120, 121**], and inhibits wild-type p53 functions in malignant melanoma [**120–122**].

The data presented in [**123**] suggests that the high levels of S100B protein found in malignant melanoma may contribute to the down-regulation of the p53 tumor suppressor via a direct S100B-p53 interaction [**122**]. This interaction may occur by S100B destabilizing p53 and/or preventing the formation of p53 oligomers, as previously observed [**116, 117, 124, 125**].

RAGE

The Receptor for Advanced Glycation Endproducts (RAGE) has been firstly described in 1992. Since then its involvement in several diseases has been extensively studied which resulted in a growing interest in RAGE as a therapeutic target [**66**]. Despite this receptor is not essential to life [**66**] it has an important role in human pathologies including diabetes, tumour outgrowth, chronic inflammation and neurodenerative disorders like Alzheimer's disease or multiple sclerosis [**66**]. In fact, RAGE signaling is very important in the inflammatory response [**107**], mediating aspects of innate immunity [**126**], acute and chronic inflammation [**127**] and certain cancers [**128**]. RAGE is up-regulated in these diseases [**129**].

RAGE is a member of the immunoglobulin (Ig) superfamily of cell surface receptors sharing structural homology with other Ig like receptors [**66**]. It consists of an extracellular moiety, a single transmembrane spanning helix and a short cytosolic domain which is required for signal transduction. The extracellular moiety includes one N-terminal V-type

and two C-type Ig domains [**67**]. Additional RAGE isoforms lacking the transmembrane and the cytosolic regions (soluble RAGE (sRAGE) for example) were identified in human brain which suggests isoform-specific functions for the receptor [**130**].

RAGE has the ability to mediate physiological and pathological effects through interaction with several ligands, each of them associated with a specific disease. Recently RAGE has been identified as a new target for several S100 proteins, including S100B [**104**].

S100B protects neurons against neurotoxic agents by interacting with RAGE. It is known that, at relatively high concentrations, S100B is neurotoxic causing neuronal death via excessive stimulation of RAGE [**131**]. S100B modulate cell survival in a RAGE-dependent manner, interacting specifically with V and C1 domains of the receptor [**132**]. It is also known that both trophic and toxic effects of extracellular S100B are mediated in the brain by the RAGE receptor [**105**].

1.3.4 S100B and Alzheimer's Disease

Alzheimer's disease (AD) is the most common form of dementia. It is characterized by the presence of deposits of amyloid-β (Aβ) peptide located extracellularly and neurofibrillary tangles, an altered intracellular arrangement of hyperphosphorylated polyubiquitinated tau protein [**133, 134**]. Metal ions, in particular zinc, iron, calcium and copper, are essential for neuronal activities and have an important role in AD. Aβ binds different metal ions, which influence its structure and amyloidogenic properties [**135, 136**].

AD has been the most extensively studied neurodegenerative disease regarding S100B pathology [**137**]. Several studies revealed that S100B protein is present in elevated levels in the brain and cerebrospinal fuid of AD patients [**104**].

In transgenic mice overexpressing S100B it was observed an enhanced susceptibility to neuroinflammation and neuronal dysfunction after infusion of Aβ. These observations support a role for S100B in AD. Moreover, recent studies in double transgenic mice overexpressing S100B and carrying a mutation in Amyloid precursor protein (APP), showed that S100B overexpression promotes brain inflammation and enhances Aβ generation from APP [**104**].

S100B might also have an important role in the formation of neurofibrillar tangles. Intracellular neurofibrillary tangles are mainly composed of hyperphosphorylated tau

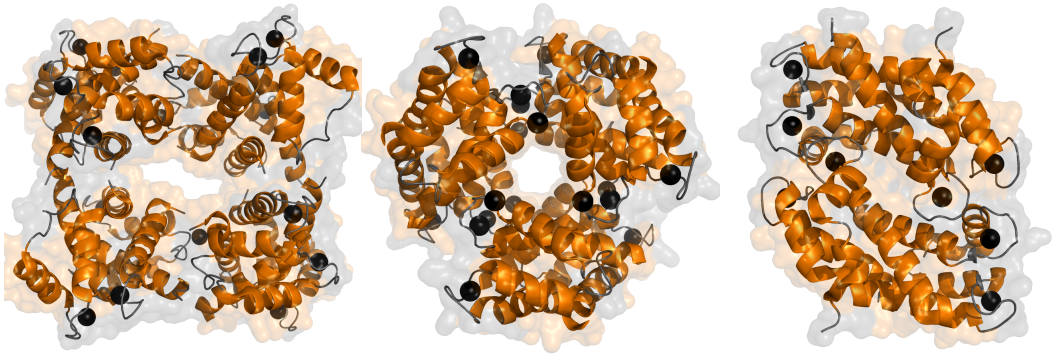

Figure 1.15: Multimeric states of S100 proteins. S100B octamer (2H61), S100A12 hexamer (1GQM), S100A8/A9 tetramer (1XK4). Image rendered using PyMOL software [**27**].

protein. S100B binds directly to tau protein in a Ca^{2+}-dependent manner. This binding results in inhibition of tau phosphorylation [**104**]. However, extracellular S100B promote RAGE-dependent hyperphosphorylation of tau protein [**104**].

These observations suggest that S100B exhibits opposite effects depending on its localization. S100B has the ability to promote the hyperphosphorylation of tau protein and has also an important role in the development of neurofibrilary tangles. These S100B capabilities are mediated by RAGE [**104**].

So, regarding all of these observations, it was hypothesized that the role of S100B in AD is mediated by RAGE [**104**].

Recent data support a novel strategy that uses S100B inhibition for reducing cortical plaque load, gliosis and neuronal dysfunction in AD. Moreover, the results obtained by Roltsch and coworkers suggest that both extracellular and intracellular S100B contribute to AD histopathology [**138**].

It is well stablished that metals like Ca^{2+}, Cu^{2+} and Zn^{2+} are present in the synaptic cleft in high concentrations [**139**]. As mentioned above they are also involved in AD, being part of Aβ plaques. These metals play a crucial role in the formation of larger oligomeric species of S100 proteins, namely tetramers, hexamers and octamers **Figure 1.15**. The formation of these oligomeric species are, in several cases, essential for biological function and signaling. S100B protein, for example, binds RAGE in the tetrameric form with higher affinity than in the dimer state. Moreover, the presence of Ca^{2+} promotes the oligomerization of S100B into hexamers and octamers. Ca^{2+} is

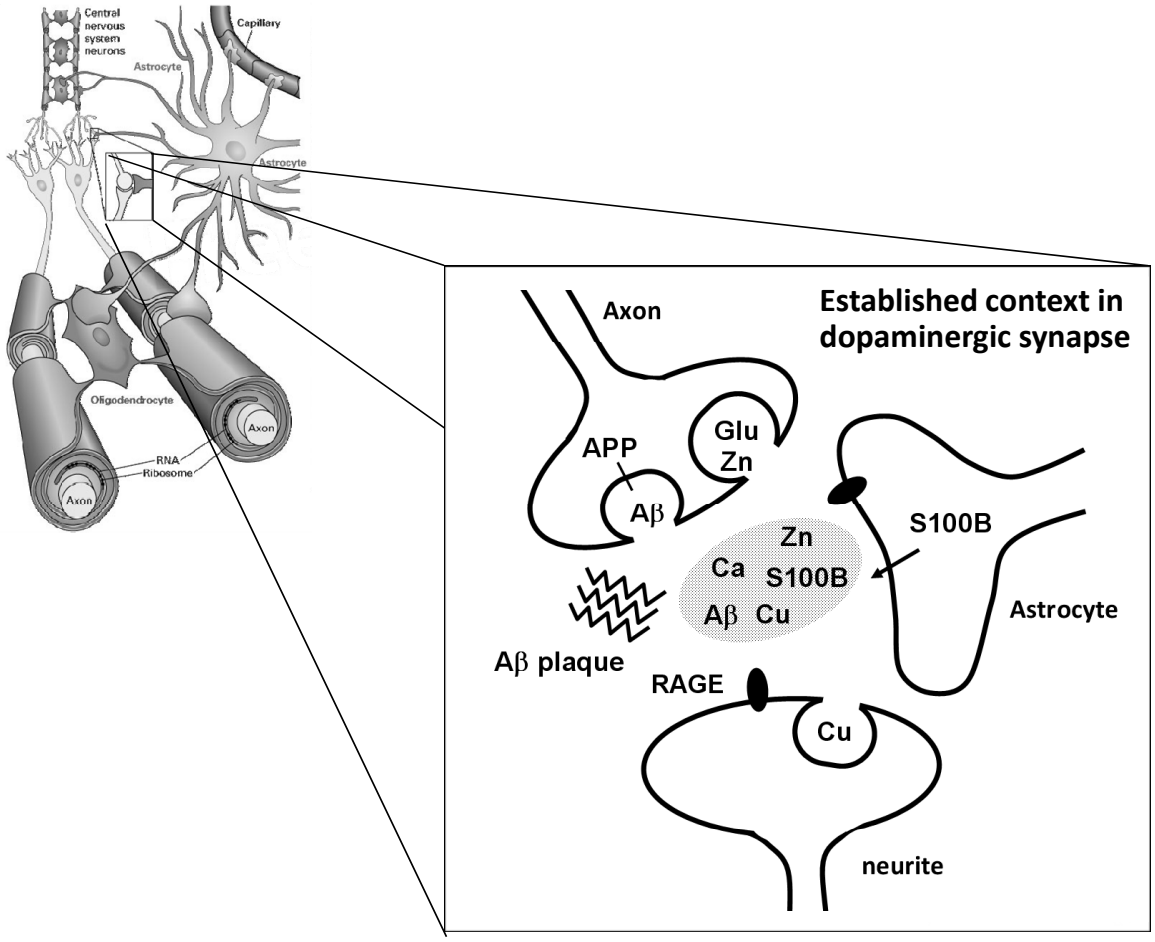

Figure 1.16: Possible involvement of S100 proteins in synaptic protein aggregation in neurodegeneration.

also responsible for the formation of the S100A8/A9 tetramer, essential to microtubule formation. Zn^{2+} has also a role in oligomerization, promoting the formation of S100A2 tetramer. Apparently metal ions have an importante role in the formation of functional S100 oligomer. Recently, it has been discovered a new property of some S100 proteins and a new role emerge: S100A8/A9 proteins can form amyloids in a metal ion mediated fibrillation process in the ageing prostate [**140**].

Several experiments performed in the host laboratory revealed a new interaction between S100B and Aβ peptide. These preliminary unpublished results showed a cross-seed effect between S100B and the Aβ peptide. S100B or Aβ amiloidogenesis is enhanced in the presence of pre-formed amyloids of the other protein.

Metallothionein-3 is an intra- an extracellular metalloprotein that is highly expressed

in the brain and downregulated in AD. This protein has the ability to protect, by an unknown mechanism, neurons from the toxicity that Aβ promotes. This toxicity is related with Cu^{2+} and Zn^{2+} interactions with this peptide. It has been reported that a metal swap between the metalloprotein and Aβ-Cu^{2+} abolishes the production of ROS and the related cellular toxicity [**141**]. This protective effect could be an important step in AD treatment, leading to new therapeutic strategies. S100B protein and this metallothionein are both expressed in the brain. The Cu^{2+}-binding to S100B have a putative neuroprotective role as described previously. These facts suggest that there are some similarities between the two proteins that can be exploited.

1.4 Objectives

Metal ions, in particular Ca^{2+}, Cu^{2+} and Zn^{2+}, have an important role in the regulation and, therefore, in the function of S100B protein. Although this role is well documented, their consequences in protein stability are not known. This fact is particularly important since S100B protein is involved in several pathological processes in which metal homeostasis is imbalanced leading to a modified protein function. This project aims to investigate the effect of metal ions on conformation and stability of protein S100B, which is essential in modulation of protein-protein interactions. Moreover, it intends to clarify the metal-dependent mechanisms by which the modulation of activity and structure of S100B protein occurs.

With this purpose were studied the wt form of human S100B as well as a mutated variant, S100B ΔCys. S100B ΔCys protein exposes less efficiently the hydrophobic core in response to binding of Ca^{2+}, which results in a weak interaction. This protein is also an important control for Zn^{2+} binding.

Chapter 2

Methodologies and Procedures

2.1 Biophysical methods to monitor protein conformational stability

The structure of a native protein is characterized by a set of unique spectral properties. During denaturation or protein conformational changes these properties undergo alterations. Therefore, they can be used to evaluate and monitor the denaturation process, by the action of chemical or physical agents. So, it is possible to monitor protein conformation and stability following the action of several destabilizing factors.

A diversity of biophysical methods are available to monitor and study the different components and characteristics of protein structure. The experimental techniques, the time scale that can be monitored and the information that can be extracted from each technique has been recently overviewed in an excellent review and is summarized in **Table 2.1**.

From the experimental data obtained by the different techniques it is possible to draw curves similar to the one represented in **Figure 2.1**, from which thermodynamic parameters of the reaction can be obtained. The midpoint transition determined from the curves, such as temperature (Tm) or concentration of chemical denaturant (Cm), is used for comparing protein stability.

The following sections will address biophysical methods used in this work to monitor protein conformation and stability .

Table 2.1: Experimental techniques useful for protein folding study. From ref. [142].

Technique	Timescale	Information content	Comments
Intrinsic tryptophan fluorescence	≥ns[a]	Environment of tryptophan (through measurement of intensity and λ_{max})	Tryptophan can be introduced (or removed to create a single-tryptophan protein) by protein engineering
Far UV CD	≥μs[a]	Secondary-structure content	Synchrotron CD may allow a more accurate interpretation of structure content. Can be complicated by aromatic contributions to the spectrum
Near UV CD	≥μs[a]	Packing of aromatic residues	Only fixed interactions give a near UV CD signal
Raman spectroscopy	≥μs[a]	Solvent accessibility, conformation of aromatic residues	Information content depends on the frequency used. Not widely applied to folding studies
Infrared spectroscopy	≥ns[a]	Secondary-structure content	Combined with solvent-exchange, information about hydrogen-exchange protection can be obtained
ANS (1-anilino-8-napthalene sulfonic acid) binding	≥μs[a]	Exposure of aromatic surface area	Care needs to be taken to ensure that ANS itself does not perturb folding
FRET	≥ps[a]	Molecular ruler, dependent on the distance between two fluorophores (r^{-6} dependence assuming free rotation of the dyes)	Information about rapid fluctuations is possible. Careful design needed to incorporate dyes without perturbing folding
FCS	≥ps	Diffusion time (and hence size and shape)	A powerful method capable of resolving co-populated conformers and their rates of interconversion over ps–ms timescales
Anisotropy	≥μs[a]	Correlation time measurements provide information about shape and size of molecule	Can provide useful complementary information to FRET distance distributions
Small-angle X-ray scattering	≥μs[a]	Radius of gyration	With modeling, information about three-dimensional structure can be obtained
Absorbance	≥ns[a]	Environment of chromophore	Peptide bond, aromatic residue or extrinsic moiety may be used
Real-time NMR	>min	Structural information via chemical shifts and measurement of NOEs	Powerful method for analysis of denatured states and intermediates in slowly folding proteins
Native-state hydrogen exchange	h	Global stability, detection of metastable states	Rare species in equilibrium with the native state that are difficult to detect using other methods can be revealed
Pulsed H/D exchange by NMR	≥ms	Hydrogen exchange protection of folding intermediates on a per-residue basis	Multiple exponential hydrogen-exchange behaviour indicates parallel pathways
Pulsed H/D exchange by ESI-MS	≥ms	Hydrogen exchange protection of folding populations	Quantification of the population of species within heterogeneous ensembles with different hydrogen-exchange properties
NMR relaxation methods	~ms	Nonrandom structure in denatured states and conformational exchange between different species	If exchange between species occurs at a suitable rate (ms), structural, kinetic and thermodynamic information about rare species can be obtained
Protein engineering	Depends on probe used	Role of an individual residue in determining the rate of folding and stability of a species of interest	Double-mutant cycles provide pairwise information. Φ-values provide indirect structural information via free-energy changes. Ψ-values use metal chelation to bihistidine motifs to identify specific side chain contacts

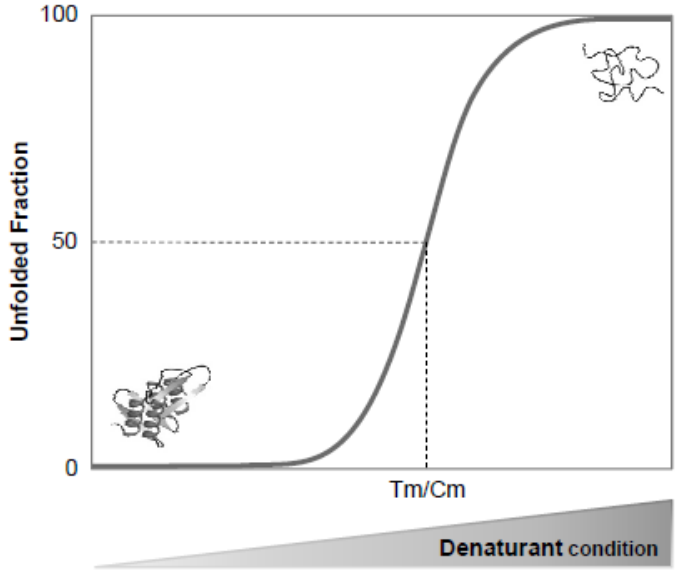

Figure 2.1: Representation of a hypothetical denaturation curve. The cartoons represent the native state (bottom) and the unfolded state (top). Tm or Cm represent temperature or chemical denaturant concentration at the midpoint of the unfolding curve. From ref. [**14**].

2.1.1 Circular Dichroism Spectroscopy

Circular Dichroism Spectroscopy (CD) is one of the methods that allows the rapid evaluation of protein folding, secondary structure content and binding properties of proteins [**143**]. CD is based on the interaction of circularly polarized light with molecular structures bearing chiral properties. In proteins these are accounted mostly by present mainly in secondary structure elements, amino acid aromatic side chains and disulfide bridges [**144**].

Proteins in the native state present a particular and characteristic CD spectrum. However, when they undergo conformational changes the CD spectrum changes, providing new information about the structure of the protein. With this method, it is possible to monitor with high sensitivity changes in secondary or tertiary structure of a protein, depending on the range of wavelengths. The secondary structure of a protein can be monitored in the far-UV region (190 to 250 nm). CD spectra have distinct shapes depending on the predominant type of secondary structure present in the protein sample **Figure 2.2**. For example, if the protein has predominantly α-helix structure it has a characteristic peak at 222 and 208 nm. However, β-sheet structures present a peak between 217 and 220 nm [**143, 145**].

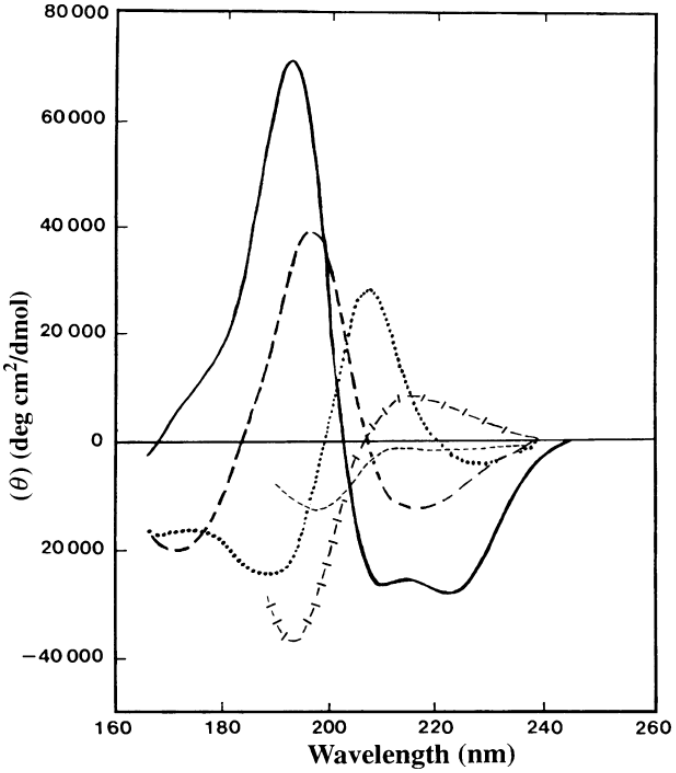

Figure 2.2: Illustration of graphs showing far-UV CD spectra associated with various types of secondary structure. Solid line, α-helix; long dashed line, antiparallel β-sheet; dotted line, type I β-turn; cross-dashed line, extended 31-helix or poly (Pro) II helix; shortdashed line, irregular structure. From ref. [**145**].

In the near-UV region (250 nm to 320 nm) it is possible to monitor tertiary structure, as this spectral region functions as a probe sensitive to environmental and topographic changes in this type of structure. CD signals in the region between 255 nm to 270 nm are assigned to phenyl groups and to phenylalanine. On the other hand, phenolic groups of tyrosine have a particular CD signal between 275 nm and 285 nm. Indole groups of tryptophan residues present a characteristic signal in the region between 285 nm and 305 nm [**146**].

CD spectroscopy has several applications and potential. It is possible, for example, study protein stability by monitoring spectrum changes induced by alterations in the environment conditions (temperature, pH, denaturant concentration) [**145**].

2.1.2 Fluorescence Spectroscopy

Fluorescence spectroscopy is a highly sensitive method used to study protein folding and dynamics through the analysis of the tertiary structure of proteins [**142**]. Most proteins have intrinsic fluorescence, a property that is due to the presence of Tryptophan (Trp), Tyrosine (Tyr) and Phenylalanine (Phe) residues. These aromatic residues allow the study of protein tertiary structure based on the measurement of intensity and wavelength emission maximum of intrinsic fluorescence of proteins. Although all of this three residues are potential natural fluorophores, Trp is the main contributor since it has the higher absortion at the emission wavelength (280 nm) and a higher emission quantum yield at a wavelength of emission ranging from 300 nm to 350 nm, depending on solvent polarity [**147, 148**]. Unlike Trp, Tyr and Phe residues are not particulary sensitive to their environment and, therefore, do not provide information about the structure of the protein. Fluorescence spectroscopy allows to evaluate the integrity of the protein tertiary structure. The higher exposure to the solvent of the aromatic aminoacids results in a deviation to higher wavelengths (deviation to red) of the emission spectra.

Besides intrinsic fluorophores we can also use extrinsic probes such Thioflavin T (ThT) and ANS (8-anilino-1-naphthalene sulfonic acid) to study folding and amyloid formation. ThT is used as a specific probe for detection of amyloid fibrils. Amyloid fibrils have a secondary structure composed primarily of β-sheets. This probe interacts with this type of structures, being interspersed with them. Thus, the connection of ThT with fibers leads to an increase in fluorescence intensity and induces a shift in the maximum wavelength from 483 nm to 478 nm [**147, 149**]. On the other hand, ANS interacts with exposed hydrophobic regions of proteins, being used to detect and characterize folding intermediates. This interaction induces a shift in the maximum emission wavelength, from 530 nm to 475 nm (wavelenght of excitation is 370 nm). Moreover, emission quantum yield increases up to 100 times after this ANS–hydrophobic region interaction[**147, 149**].

2.1.3 Dynamic Light Scatering

Dynamic Light Scattering (DLS), is a technique used to characterize the size and the size distribution of biomolecules in solution. It is a relatively fast method (it only takes a few minutes to perform a measurement) and allows the analysis of particles with sub-micrometric sizes [**150**].

When a light source illuminates a solution, the particles present in this solution will

scatter the light in all directions. This method analyses the intensity and the fluctuations of the scattered light and is able to detect them due to the Brownian motion of molecules in solution [**150**]. Brownian motion is the movement of particles due to random collision with the molecules of the liquid that surrounds the particle.

DLS works without exact knowledge of the sample concentration and has been used with success in structural biology. The only requirement is that enough light must be scattered to achieve sufficient statistical accuracy [**150**]. It should be noted that this is a method with low resolution so in order to have a distinct separation between two species they have to be different in terms of molecular mass. Therefore, DLS is more appropriate to use in aggregates with large sizes than in small oligomers [**151**].

2.1.4 Measuring the conformational stability of a protein

In order to measure the conformational stability of a protein it is necessary to determine the equilibrium constant and the free energy change, ΔG for the following reaction:

$$F \rightleftharpoons U \tag{2.1}$$

Usually, the conformational stability is called $\Delta G(H_2O)$ at 25°C, where H_2O represents the absence of a denaturant. There are several techniques that can be used to follow the unfolding of a protein: UV difference spectroscopy, fluorescence and CD are the most used. The choice of technique depend on several factors that will determine whether it is right for the system under study. Although a particular method can be more informative, it may require more material or be very expensive, which conditions the choice. One should take into account three factors: i)The magnitude of the response may be of crucial importance. Different techniques require different amounts of protein, which is an important factor during the choice; ii)It is necessary to pick a technique and a wavelenght for which the spectra/characteristics of the folded and unfolded conformations differ significantly; iii)Another important factor is the signal-to-noise ratio. The greater its value the more accurate the measurements.

Figure 2.1 shows a typical unfolding curve. It is possible to divide this type of curves in three regions. Pre–transition region, that shows how the signal of folded protein depends upon the denaturant; transition region, that shows how the signal change as unfolding occurs and post–transition region, that shows how signal of unfolded protein varies with

denaturant.

Measuring the conformational stability of a protein implies thermodynamic measurements. So, it is essential that the unfolding reaction has reached equilibrium before measurements are made and that the unfolding reaction is reversible. The unfolding of many monomeric globular proteins has been found to closely approach a two–state folding mechanism (see eq1). However, there may be intermediates and the folding mechanism becomes one of three states. In the next lines it will be assumed a model of two states, in order to facilitate the discussion. So, for a determined temperature:

$$f_{\mathrm{F}} + f_{\mathrm{U}} = 1 \tag{2.2}$$

Where f_{F} and f_{U} represent the fraction of molecules in the folded and in the unfolded conformation, respectively. Thus, the observed value of y at any point will be:

$$y = y_{\mathrm{F}} f_{\mathrm{F}} + y_{\mathrm{U}} f_{\mathrm{U}} \tag{2.3}$$

where y_{F} and y_{U} represent the values of y characteristic of the folded and unfolded states, respectively.

Combining these two equations yields:

$$f_{\mathrm{U}} = \frac{y_{\mathrm{F}} - y}{y_{\mathrm{F}} - y_{\mathrm{U}}} \tag{2.4}$$

The equilibrium constant, K, and the free energy change, ΔG, can be calculated using:

$$K = \frac{f_{\mathrm{U}}}{1 - f_{\mathrm{U}}} = \frac{f_{\mathrm{U}}}{f_{\mathrm{F}}} = \frac{y_{\mathrm{F}} - y}{y - y_{\mathrm{U}}} \tag{2.5}$$

and

$$\Delta G = -RTlnK = -RTln\frac{y_{\mathrm{F}} - y}{y - y_{\mathrm{U}}} \tag{2.6}$$

where R is the gas constant and T the absolute temperature. It should be noted that values of y_{F} and y_{U} are obtained by extrapolating from the pre- and post-transition regions.

Thermal unfolding

The analysis of thermal unfolding curves require ΔG measurements from the narrow temperature range where unfolding occurs to an ambient temperature. The method used to obtain the enthalpy change is the van't Hoff equation:

$$\frac{\mathrm{d}(lnK)}{\mathrm{d}(1/T)} = -\frac{\Delta H}{\mathrm{R}} \tag{2.7}$$

Entalphy change varies with temperature, which is expected when the heat capacities of the products and reactants differ:

$$\frac{\mathrm{d}(\Delta H)}{\mathrm{d}(T)} = \mathrm{C_p(U)} - \mathrm{C_p(F)} = \Delta \mathrm{C_p} \tag{2.8}$$

It is necessary both ΔC_p and ΔH to calculate ΔG as a function of temperature. ΔH is needed at only a single temperature, and the best to use is T_m, the midpoint of the thermal unfolding curve, where $\Delta G(T_m) = 0$.

With these parameters we can calculate ΔG at any temperature:

$$\Delta G(T) = \Delta H_m(1 - T/T_m) - \Delta \mathrm{C_p}[(T_m - T) + Tln(T/T_m)] \tag{2.9}$$

Irreversible thermal denaturation

All the formalism described above is only valid for a reversible thermal denaturation. However, thermal unfolding denaturation can be an irreversible process. It is not possible to derive directly thermodynamic parameters from irreversible systems, as these are under kinetic control. The irreversible thermal denaturation of a protein comprises at least two steps: the reversible unfolding of the native protein to the denaturated form, followed by a kinetically controlled step, leading to a final irreversible state. It was developed a formalism that allow to be established that the kinetic effects are reflected in the scan rate dependency of the observed transitions and that these become negligible at sufficiently high scan rates, ultimately at an infinite scan rate. Under these conditions, the contribution of the irreversible step is eliminated and the observed transition reflects exclusively the reversible component of the process, from which thermodynamic parameters can be obtained [**152**].

In this work, there are irreversible thermal denaturation transitions. For these processes, the thermodynamic parameters calculated are named as apparent. So, instead of T_m values we used the onset point of aggregation, named T_{agg}, which is the temperature at which the protein aggregation starts. It should be noted that, even with apparent parameters, they are quite useful for comparing experiments performed under the same conditions.

2.2 Materials and Methods

2.3 Chemicals

All reagents were of the highest grade commercially available. All solutions were prepared in water treated with the chelating material Chelex(Sigma-Aldrich). The buffers used were oxygen-free.

2.4 Protein Expression and Purification

Wild type S100B and the mutant ΔCys (cysteine deficient variant(C68S-C84S)) were expressed in *E.coli* BL21(DE3) and purified to homogeneity, as previously described [**153**]. The plasmids and the first cellular extracts for both proteins were provided by our collabolator Guenter Fritz.

2.4.1 S100B Expression

The cDNA for human S100B was cloned into expression vector pGEMEX–2 (ampicilin resistance). S100B protein was expressed in *E.coli* BL21(DE3).

Bacterial cells were grown at 37°C in 50 mM phosphate-buffered DYT medium pH 7.4 containing 0.2% glucose. The expression was induced by the addition of 1 mM of IPTG at an optical density OD_{600} nm of 0.6 and the culture was grown overnight. Cells were harvested by centrifugation at 8000 rpm for 10 min.

2.4.2 S100B Purification

S100B protein undergo a conformational change upon Ca^{2+}-binding that exposes a hydrophobic core. Based on this property the purification was performed in two steps,

using Ca^{2+}-dependent Hydrophobic Interaction Chromatography and subsequent Size Exclusion Chromatography.

For protein purification, 10 g of cells were suspended in 20 mL 50 mM Tris-HCl, 5 mM $MgCl_2$ pH 7.6. A few crystals of DNAse I were added and cells were broken by three passages through a French press. After cell breakage, 0.5 mM PMSF was added and the crude extract was centrifuged at 18000 g for 35 min. A second centrifugation was performed at 42000 rpm for 45 min. The supernatant was diluted 2-fold with 50 mM Tris-HCl pH 7.6 and 5 mM $CaCl_2$ was added. The diluted supernatant was then loaded onto a phenyl-Sepharose Fast Flow Column (Amersham, GE-Healthcare) equilibrated with 50 mM Tris-HCl, 5 mM $CaCl_2$ pH 7.6. The column was washed with 20 volumes of the same buffer until absorption at 280 nm reached a baseline. For S100B ΔCys, since it contains cysteines, 0.5mM was added to the wash buffer. Bound S100B protein was eluted with 50 mM Tris-HCl, 10 mM EDTA pH 7.6. The obtained protein was concentrated by ultrafiltration and loaded onto a Superdex 75 column (Amersham, GE-Healthcare) equilibrated with 20 mM Tris-HCl, 150 mM NaCl pH 7.6.

The two proteins obtained were concentrated to 20 mg/mL by ultrafiltration with Amicon centricons with a 3 kDa cut-off. The aliquots were flash frozen in liquid nitrogen.

In order to evaluate the purity of the protein it was performed a 12% acrylamide SDS-PAGE gel and were traced far-UV CD (from 190 to 260 nm)and UV-visible (from 250 to 800 nm) spectra.

S100B protein concentration was determined spectrophotometrically using the visible absorption extinction coefficient ϵ^{280}=1490 $M^{-1}.cm^{-1}$. This was performed using a Shimadzu UV-1700 spectrophotometer at room temperature.

For all subsequent experiments protein concentration used was 0.15 mg/mL (14 μM). The buffer used was 20 mM Tris-HCl pH 7.0.

Previous studies have determined that the cysteine to serine substitutions in S100B ΔCys do not compromise the overall fold but only a small part of helix H_{IV} 1.3. Posterior to the experiments performed during this work the structure of S100B ΔCys was resolved and was noticed that it had zinc bonded. Zinc was used during protein purification and apparently it stayed bonded even with the addition of EDTA. This fact explains several results and should be taken into account for the future work.

2.5 Preparation of apo S100B wt

Prior to all experiments S100B wt protein was incubated with a 300-fold excess of DTT for 2 h at 37 °C to reduce all cysteine residues. Metal ions were removed by addition of 0.5 mM EDTA [**79**]. Both EDTA and DTT were removed on a Desalting column (GE Healthcare) equilibrated with the chosen buffer. It was concentrated by ultrafiltration and quantified spectrophotometrically as mentioned above (see section 2.4).

2.6 Preparation of metal loaded proteins

There were prepared several protein samples with and without metal ions. To apo protein were added 0.5 mM of EDTA or 140 μM (10 molar equivalents) of metal ions , $CaCl_2$, $ZnCl_2$, $CuSO_4$. Unless otherwise indicated, all measurements were done immediately after the addition of EDTA or metal ions.

2.7 Circular Dichroism Spectroscopy

CD measurements were recorded in a Jasco J-815 spectropolarimeter equipped with a Peltier-controlled thermostated cell suport using a quartz cuvette of 1 cm. The far-UV CD spectra were traced in a wavelength range from 190 to 260 nm with the following parameters: 200 nm/min of speed (continuous mode), 2 nm of bandwidth, 1 s of response and an average of 10 accumulations. These spectra were acquired at 25°C, before and after heating as well as at 90/95/99°C. Temperature Ramps were done following the wavelength 222 nm. The other parameters were: 100 mdeg of sensibility, 2 nm of bandwidth and 1 s of response. Temperature was increased in at a rate of 1°C/min in a range from 25 to 90, 95 or 99°C.

2.7.1 Metal Binding Competition Experiments

Zn^{2+} or Cu^{2+} were added to apo wt and ΔCys protein and far-UV CD-spectra were traced at 25°C. The samples were incubated during 1 h and another spectra were traced. After this the second metal was added (Cu^{2+} or Zn^{2+}) and a new spectra were done. For the two-metal-loaded protein samples thermal denaturation was performed in a 25-95°C range. Far-UV CD spectra were also performed at 95°C and after the sample was cooled until 25°C .

2.7.2 Zinc Binding Kinetics

Zn^{2+} was added to apo wt and ΔCys protein and far-UV CD-spectra were traced every five minutes during 2 h at 25°C.

2.8 SDS-PAGE and Native-PAGE

The SDS- and Native-PAGE analysis were performed using 15% acrylamide gels with Mini-Protean 3 system, from Bio-Rad. The samples were prepared by adding 50% (v/v) of loading buffer and, only in the case of SDS-PAGE, incubated at 100°C for 10 minutes. The SDS-PAGE Molecular Weight Markers used were from Amersham Biosciences (Low Molecular Weight Calibration Kit for SDS Electrophoresis). Gels were eluted at 200 V, were stained with Comassie Blue (USB Corporation) and bleached with an aqueous solution of acetic acid (5%) and methanol(10%).

2.8.1 TCEP assays

Samples were incubated 1h at 37°C with 5 mM TCEP and β-mercaptoetanol.

2.9 Fluorescence Spectroscopy

Intrinsic tyrosine measurements of S100B protein were performed on a Varian Cary Eclipse instrument. Temperature was kept at 25°C by a Peltier-controlled cell support. Emission spectra upon 275 nm excitation were recorded using 10 nm excitation and emission slits.

S100B protein does not have Trp residues and only have one Tyr which has a low quantum yield. The measurements performed do not allow to distinguish between the native state and denatured state (data not shown). Therefore, the studies using this technique did not proceed.

2.10 Dynamic Light Scattering

The molecular diameter of S100B protein at 0.15 mg/mL was assessed using a Malvern Instruments Zetasizer Nano ZS instrument equipped with a 633 nm laser. Temperature was increased in a range between 25°C and 95°C and controlled using a Peltier-controlled

thermostatized cell support. Before each measurement, samples were filtered through a 0.22 μM membrane. Results were analyzed with Malvern Instruments DTS software.

During DLS experiments protein stock ended so it was not possible to perform a complete study of S100B wt and ΔCys protein in several metal-loaded states.

Chapter 3

Results and Discussion

3.1 Metal binding to S100B induces structural changes

S100B protein has the ability to bind Ca^{2+}, Cu^{2+} and Zn^{2+}. Metal ions play an important role in structure and, therefore, in the function of S100B protein. Thus, it becomes important to understand metal-binding mechanisms and how do they induce conformational changes in this S100B.

In order to investigate the effect of metal ion binding on the structure of S100B, the *wild type* (*wt*) and a cysteine-to-serine mutant, ΔCys protein, were studied in apo (metal free) and holo (metal loaded) forms. These conformational studies were performed using far-UV circular dichroism (CD). S100B *wt* and ΔCys proteins samples were prepared in several metal load conditions. In addition to apo protein, Ca^{2+}, Cu^{2+} and Zn^{2+}metal ions were added to different samples . Moreover, addition of EDTA was used as a negative control.

It should be noted that, as mentioned previously (section 1.3), the replacement of cys by ser does not affect the overall fold nor the Ca^{2+} affinity.

The CD spectra of all protein preparations at 25°C are typical of α-helix proteins (**Figure 3.1**). However, the intensity of the spectra and, therefore, the content on secondary structure, depends on the protein (S100B *wt* or ΔCys) and on metal load conditions.

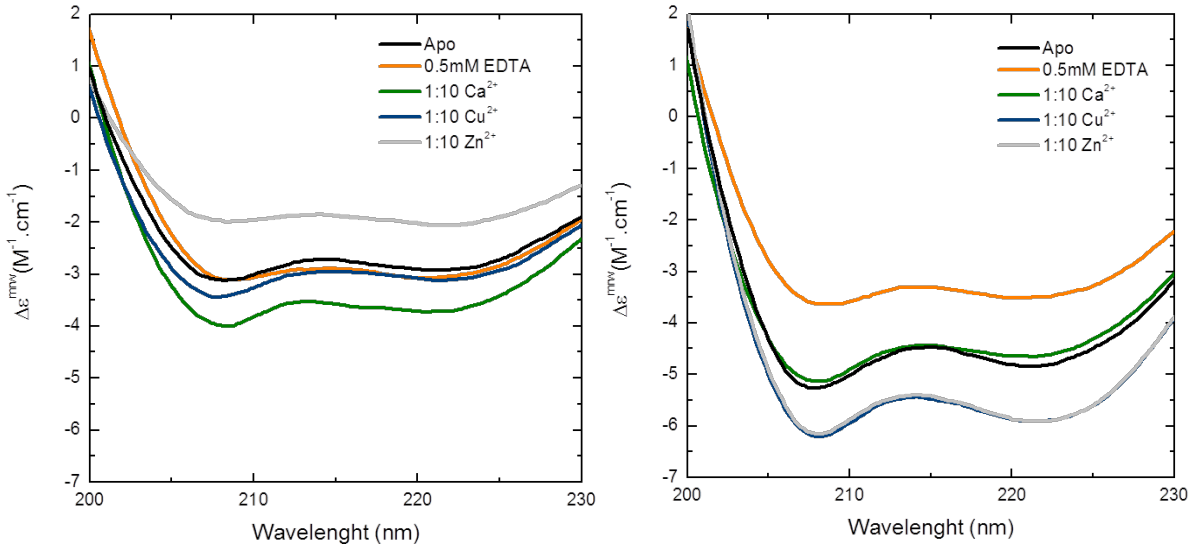

(a) S100B wt **(b)** S100B ΔCys

Figure 3.1: CD-monitored S100B conformational changes upon metal binding Representative CD spectra of S100B *wt* (a) and ΔCys (b) in several metal load conditions: apo(black line), Ca^{2+} (green line), Cu^{2+} (blue line), Zn^{2+} (grey line) and EDTA (orange line)

Conformational changes induced by metal ions on S100B *wt*

CD spectra of S100B wt protein (**Figure 3.1a**) show that the addition of EDTA to S100B *wt* apo protein does not elicit significant secondary structure changes. EDTA addition was a negative control used to make sure that the apo sample is free of metals. CD spectra corroborates that. However, after metal binding the far-UV CD spectra of the protein undergo changes. Cu^{2+}-binding induces a small increase in secondary structure content, but is upon Ca^{2+}-binding that the increase in α-helical content is higher. On the other hand, Zn^{2+}-binding has the opposite effect observed for Ca^{2+} and Cu^{2+}, as it significantly decreases the secondary structure of the S100B. It is known that Ca^{2+}-binding to S100B protein induces conformational changes, which is corroborated by CD spectra of **Figure 3.1a**. At 25°C, Zn^{2+} decreases the content of secondary structure but Cu^{2+} does not have a significant effect.

Conformational changes induced by metal ions on S100B ΔCys

S100B ΔCys presents a different behaviour when compared to S100B wt (**Figure 3.1b**). In this case, far-UV CD-spectrum of S100B ΔCys apo protein is quite different from the negative control (EDTA). Upon EDTA addition, it is observed a significant decrease in secondary structure content. This can be justified because S100B ΔCys apo, as was discovered recently (see section 2.4), has Zn^{2+} bonded. Zn^{2+} stabilizes the α-helix H_{IV} so the apo sample has a different intensity in far-UV CD spectrum. Altough EDTA was not able to remove all the Zn^{2+} ions during protein purification, it can remove some metal ions from S100B ΔCys, leading to a decrease in far-UV CD spectrum signal. Ca^{2+} binding gives rise to a spectrum very similar with the apo protein one, being only slightly less intense. Binding of Cu^{2+} and Zn^{2+} to the protein results in a conformational change inducing the highest increase in α-helical content. The two spectra are completely overlapped which makes sense if we take into account that the binding sites for these ions are the same.

It should be noted that for S100B *wt* protein the binding of Cu^{2+} and Zn^{2+} does not elicit the same conformational changes, at least in terms of signal intensity. Therefore, for the S100B *wt* protein there could exist another factor that makes this metal-binding effect change.

In general, the content of secondary structure of S100B *wt* protein is lower than the one for S100B ΔCys. This may due to the fact that the S100B *wt* protein requires preparation (section 2.5) before experiments and this manipulation may introduce minor

destabilization on protein. Therefore, the intensity of the S100B *wt* and ΔCys spectra should not be compared.

3.2 Cu^{2+} and Zn^{2+} binding to S100B decreases thermal stability

Metal binding to S100B protein induces not only conformational changes but affects also the stability of the protein. The conformational stability of S100B *wt* and ΔCys, in the apo and distinct metallated states was investigated by temperature-induced unfolding assays. Temperature of thermal denaturation experiments was modified in the 25-90/95/99°C range. The far-UV CD-spectra were traced at 25°C, before and after heating and also at 90/95/99°C.

3.2.1 Thermal stability of native S100B

The T-Ramp of S100B *wt* apo and the negative control (EDTA) samples are overlapped and is not visible any transition (**Figure 3.2f**). Moreover, the far-UV CD spectra of both samples present the same behaviour (**Figure 3.2a** and **Figure 3.2b**) . The 90°C and 25°C cooled spectra suggest a conformational change: a loss of α-helical content and a gain of β-sheet secondary structure. Although not completely identical, the S100B protein loaded with Ca^{2+} has a very similar behavior with that of the previous samples. The T-Ramp has a visible transition and is not overlapped with the other two. However, the conformational changes induced by thermal denaturation are, apparently, the same(**Figure 3.2c**). Ca^{2+} induces a conformational change in S100B protein which can explain the presence of a transition in the T-Ramp of Ca^{2+}-loaded protein. For these three protein samples there was no evidence of aggregates. The T-Ramp and the CD-spectra of Cu^{2+} and Zn^{2+}-loaded samples are different from the ones described above (**Figure 3.2d**, **3.2e** and **3.2f**). The far-UV CD spectra after thermal denaturation (95°C/99°C and 25°C cooled sample) (**Figure 3.2d** and **3.2e**) indicate a total denaturation of protein. The CD signal intensity is almost zero, which represents loss of α-helix secondary structure. The T-Ramps of both samples present a well-defined transition. For these samples it was observed a large amount of aggregates, which is in agreement with the CD spectra measured after denaturation. As mentioned in section 2.1.4 it is not possible to calculate the Tm for thermal unfolding irreversible systems. In this case, we will use the temperature of aggregation (T_{agg}) instead of Tm. For Cu^{2+}

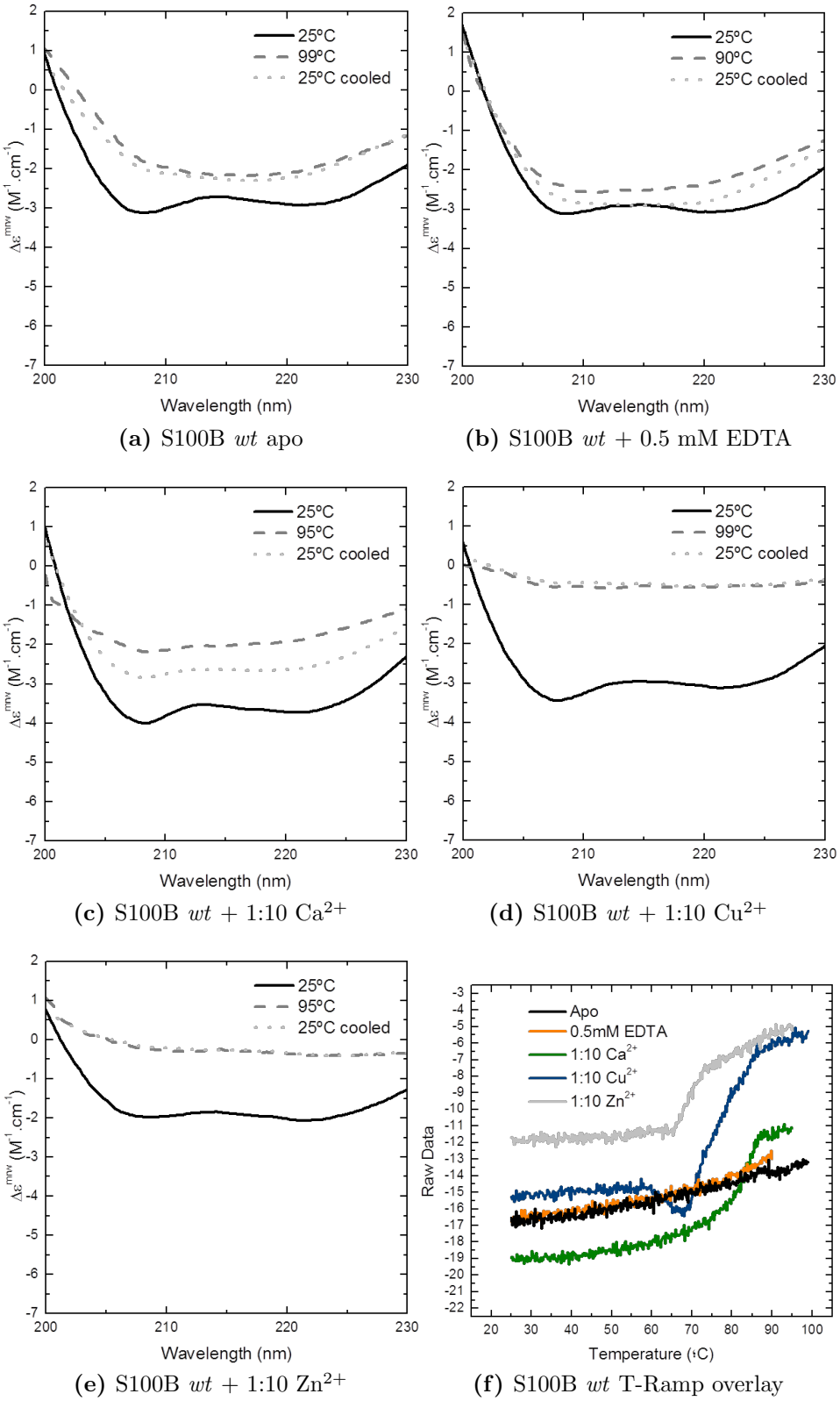

(a) S100B *wt* apo **(b)** S100B *wt* + 0.5 mM EDTA

(c) S100B *wt* + 1:10 Ca^{2+} **(d)** S100B *wt* + 1:10 Cu^{2+}

(e) S100B *wt* + 1:10 Zn^{2+} **(f)** S100B *wt* T-Ramp overlay

Figure 3.2: CD-monitored thermal denaturation of S100B *wt*. Representative spectra at different temperatures in several metal load conditions (a)-(e); T-Ramp overlay in several metal load conditions (f).

and Zn^{2+} loaded samples the T_{agg} is 68°C and 65°C, respectively. As S100B wt apo protein does not present a transition, we can not compare its Tm with T_{agg} for Cu^{2+} and Zn^{2+} samples. However, we can conclude that S100B wt protein is more stable in the apo state than when it is loaded with Cu^{2+} or Zn^{2+}, as for the first case it does not aggregate. The study of thermal stability of holo and apo S100B *wt* suggests that the different samples can be separated into different groups. Holo samples do not present aggregates after thermal denaturation which make possible a kind of reversibility. After heating the samples they do not unfold but suffer a conformational change instead. Ca^{2+}-loaded S100B *wt* suffers a conformational change before heating, which is translated into a visible transition in T-Ramp. However, the Ca^{2+}-induced conformational change does not influence the presence of aggregates. Cu^{2+} and Zn^{2+}-loaded samples can be considered an individual group since both of them form aggregates after thermal denaturation and the CD spectra show that protein does not have the ability to recover the fold after heating. The binding of these two metals apparently induce a large conformational change that alters the stability of the protein.

3.2.2 Thermal stability of S100B ΔCys

The thermal stability study of S100B ΔCys upon metal binding reveals a similar behaviour when compared with S100B *wt* protein. S100B ΔCys apo and Ca^{2+}-loaded are samples very similar between them. The addition of EDTA does not induce significant changes. The three T-Ramps present the same shape and are only different in terms of signal intensity, which is normal if we take into account the CD spectra at 25°C. Moreover, these T-ramps do not present any visible transition (**Figure 3.3f**). After thermal denaturation these samples have the ability to recover some secondary structure content. In fact, after denaturation it is visible some reversibility in CD spectra, however, protein suffers a conformational change, which is reflected in an increase of β-sheet secondary structure. These changes that protein undergoes are visible in the CD spectra of samples after heating and after cooling (**Figure 3.3a**, **3.3b** and **3.3c**). Despite this conformational change, apo and Ca^{2+}-S100B ΔCys samples do not present aggregates after thermal denaturation. The negative control does not present protein aggregation also. Again, as occurs in S100B wt protein, Cu^{2+} and Zn^{2+} samples could be inserted into a different group since they present a different behaviour in these experiments. The thermal denaturation profile are different from the other samples as well as the capacity of reversibility (**Figure 3.3f**). S100B ΔCys loaded with Cu^{2+} and Zn^{2+} form aggregates and do not present α-helix content in far-UV CD-spectra at 90°C

and 25°C cooled (**Figure 3.3d** and **3.3e**). In fact, these two spectra have an intensity near zero suggesting that the protein is denaturated. Thermal denaturation ramp of Cu^{2+}-loaded protein exhibit a visible transition and the T_{agg} =80°C. The Zn^{2+} sample present a very well defined transition profile in T-Ramp but the T_{agg} is lower, 69°C.

The main observations that can be taken from these results are that altough S100B wt and ΔCys protein undergo a conformational change upon Ca^{2+} binding this not affect the stability of the protein. Moreover, thermal denaturation does not induce the formation of aggregates but converts some of the α-helix content in β-sheet secondary structure. On the other hand, Cu^{2+} and Zn^{2+} binding to S100B protein induce a large conformational change, which is reflected in terms of stability. Upon Cu^{2+} or Zn^{2+} binding, thermal denaturation experiments showed that the protein tends to denaturate and aggregate. Although thermal stability of S100B wt loaded with Cu^{2+} or Zn^{2+} is not very different, the S100B ΔCys protein presents almost 15°C of difference. For this last protein, Cu^{2+} is much more stable than Zn^{2+}.

3.3 Copper and Zinc have different effects on S100B structure and stability

The results of the previous section showed that Cu^{2+} and Zn^{2+} binding to S100B protein have a different effect in conformation and stability. The behaviour presented by the samples loaded with these two metals was quite different from Ca^{2+}-loaded or apo protein. So, in order to better understand the role of these metals in protein structure and stability a new set of experiments was done. It has been reported that the binding of Cu^{2+} and Zn^{2+} frequently occurs at the same binding sites, but with different affinities. These new CD experiments pretended to study Cu^{2+} and Zn^{2+} binding competition and to clarify their role together on S100B structure and stability.

3.3.1 Effect on S100B secondary structure

The structural changes induced by Cu^{2+} and Zn^{2+} on S100B protein were studied by performing far-UV CD-spectra. For S100B wt and ΔCys proteins each metal ion was incubated for 1 h and then the second metal was added.

The wt protein loaded with Zn^{2+} does not loss signal in far-UV CD spectrum, even after 1 h of incubation. However, when Cu^{2+} is added to this sample, it is observed a

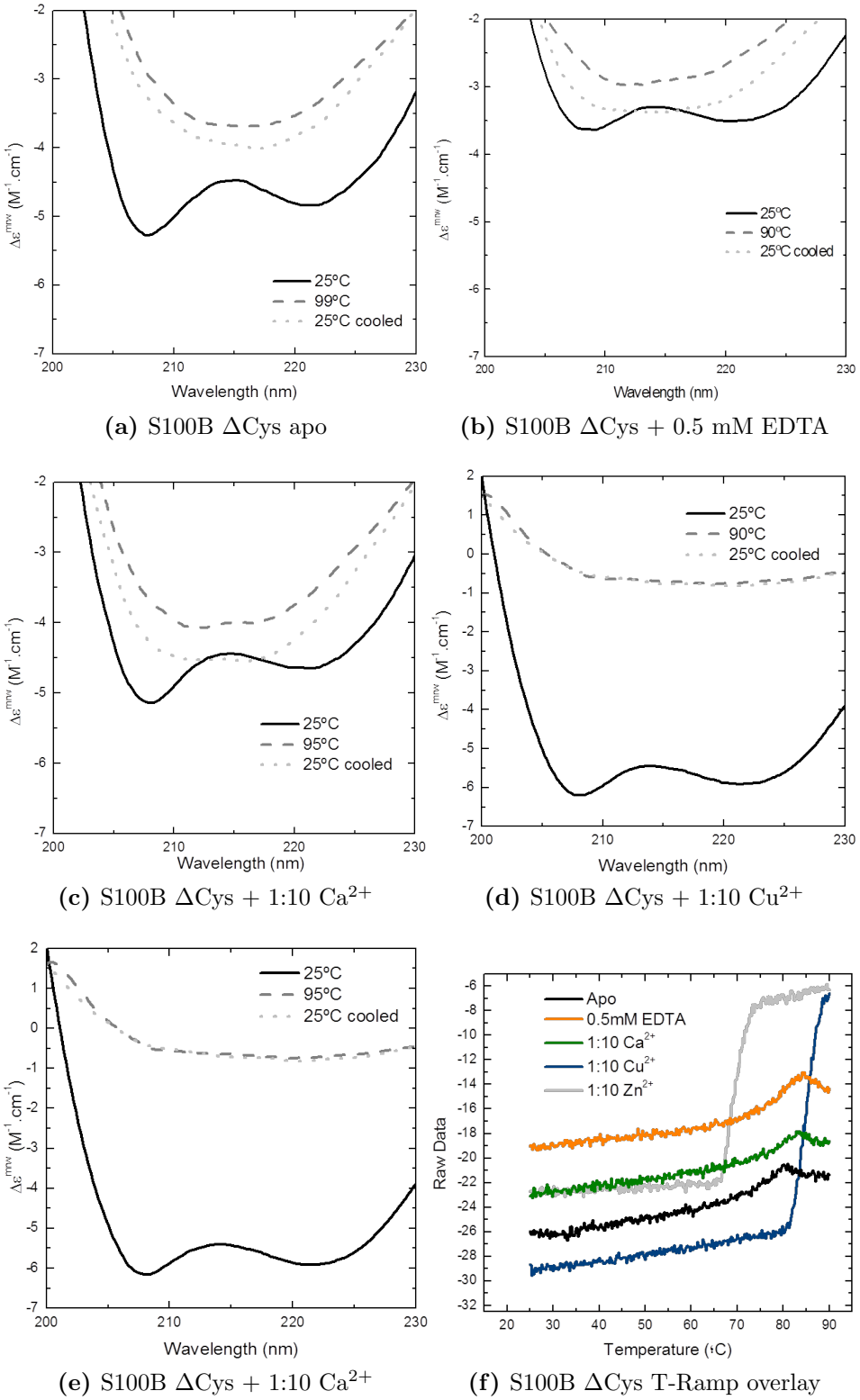

(a) S100B ΔCys apo

(b) S100B ΔCys + 0.5 mM EDTA

(c) S100B ΔCys + 1:10 Ca^{2+}

(d) S100B ΔCys + 1:10 Cu^{2+}

(e) S100B ΔCys + 1:10 Ca^{2+}

(f) S100B ΔCys T-Ramp overlay

Figure 3.3: CD-monitored thermal denaturation of S100B ΔCys. Representative spectra at different temperatures in several metal load conditions (a)-(e); T-Ramp overlay in several metal load conditions (f).

conformational change, indicated by a decrease in α-helical content (**Figure 3.4a**). On the other hand, the incubation of 1 h with Cu^{2+} results in a significant loss of α-helix signal (**Figure 3.4b**). The later addition of Zn^{2+} does not present any changes when compared to the 1h incubated sample.

S100B ΔCys incubation for 1h with Zn^{2+} gives rise to a significant loss of signal, which indicates a decrease in α-helical content (**Figure 3.4c**). Nevertheless, the signal of far-UV CD spetrum increases upon Cu^{2+} binding, but not to the initial values. Cu^{2+} incubation and later addition of Zn^{2+} to ΔCys protein does not affect significantly the secondary structure content (**Figure 3.4d**).

These results suggest that Cu^{2+} has the ability to displace Zn^{2+} from his binding site and that the effects of these two metal ions are different, depending on the protein. For S100B wt, Zn^{2+} incubation does not affect the stability of the protein. However, Cu^{2+} has a destabilizing effect and is able to exert that because can displace Zn^{2+}. Zn^{2+} is not able to displace Cu^{2+} and his effect is not visible if the sample has already Cu^{2+}. On the other hand, for S100B ΔCys protein the metal ions effect is the opposite. Zn^{2+} incubation is destabilizing and Cu^{2+} has a stabilizer effect. Moreover, Cu^{2+} has also the ability to displace Zn^{2+} from the binding site.

3.3.2 Effect on S100B thermal stability

In order to study the Cu^{2+} and Zn^{2+} binding competition on S100B stability T-Ramp experiments with the two metals were done.

The T-Ramp of S100B *wt* protein loaded with Zn^{2+} presents a T_{agg} around 65°C (**Figure 3.5a**). However, when it has Zn^{2+} and Cu^{2+} bonded, protein aggregation begins sooner, at 30°C. As the two metal loaded T-Ramp does not present a visible transition, the T_{agg} was estimated taking into account the increase in High Tension Voltage, an indicator of aggregation (data not shown). It should be noted that the shape of the two T-Ramps is very different, which is reflected in protein stability . The far-UV CD spectra of Zn^{2+} and Cu^{2+} loaded sample after thermal denaturation are typical of β-sheet secondary structure (**Figure 3.4a**). Apparently, although Zn^{2+} + later Cu^{2+} addition sample is less stable, after heating it presents an higher content in secondary structure, when compared with Zn^{2+}-loaded S100B *wt* protein. This is curious because Cu^{2+} destabilizes S100B wt protein.

S100B *wt* loaded with Cu^{2+} starts to aggregate, during thermal denaturation, at 68°C.

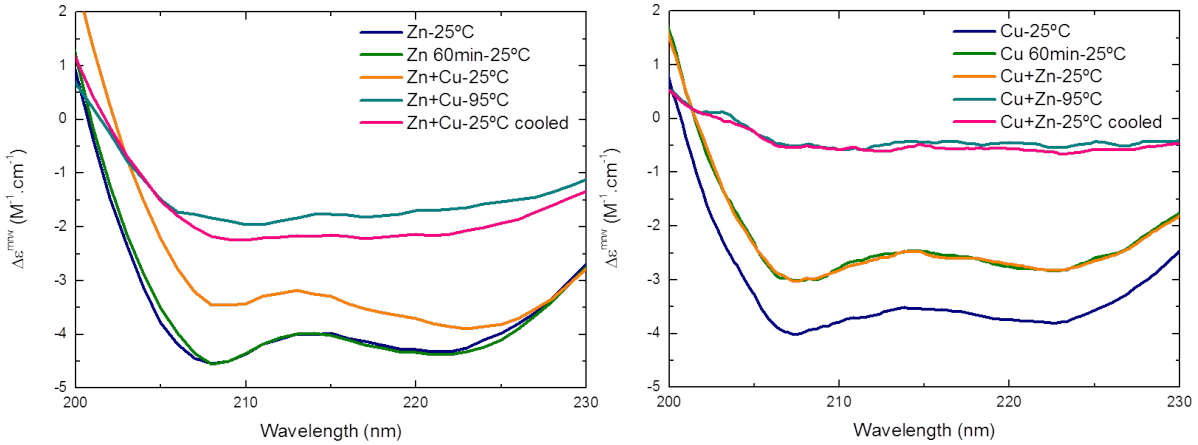

(a) S100B *wt* loaded with Zn^{2+} + later Cu^{2+} addition

(b) S100B *wt* loaded with Cu^{2+} + later Zn^{2+} addition

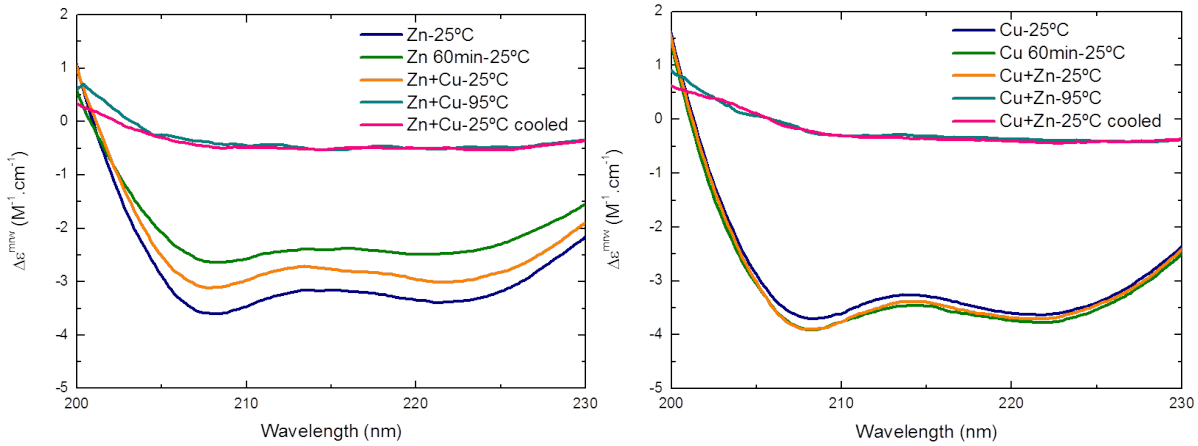

(c) S100B ΔCys loaded with Zn^{2+} + later Cu^{2+} addition

(d) S100B ΔCys loaded with Cu^{2+} + later Zn^{2+} addition

Figure 3.4: Metal binding competition on S100B structure. Representative CD Spectra of S100B *wt* and ΔCys loaded with Cu^{2+} and Zn^{2+} metal ions.

When Zn^{2+} is added to this sample T_{agg} changes to 40°C (**Figure 3.5b**). In this case, the shape of the T-Ramps are more similar than the anterior one. However, the stability of the two samples are very different. Moroever, contrary to what happened to the sample loaded with Zn^{2+} + later Cu^{2+} addition, the CD spectra at 95°C and 25°C cooled have an intensity near zero which suggests that the protein is totaly unfolded (**Figure 3.4b**). Zn^{2+} addition induces a decrease in thermal stability and makes impossible a recovery of secondary structure.

When S100B ΔCys loaded with Zn^{2+} is submitted to thermal denaturation, it starts to aggregate at 66°C. Nevertheless, the consequent addition of Cu^{2+} changes the stability. In this case, the T_{agg} is 71°C (**Figure 3.5c**). The two T-Ramps are very similar, which not occurs in S100B *wt* samples. After heating the CD signal decreases to values near zero, so the protein is in the denaturated state (**Figure 3.4c**).

S100B ΔCys protein loaded with Cu^{2+} has a T_{agg} near 80°C (**Figure 3.5d**). However, when Zn^{2+} is added the aggregation during thermal denaturation starts at 74°C. Once again the 95° and 25°C cooled CD spectra present values near zero (**Figure 3.4d**).

The effect of Cu^{2+} and Zn^{2+} binding on S100B structure and stability, in particular the results presented in this section, are resumed in **Figure 3.6**. Taking into account these results, it can be considered that Cu^{2+} binding to S100B affects the conformation of S100B protein but not of S100B ΔCys. Moreover, for S100B protein, subsequent Zn^{2+} addition has no effect on folding but it affects the stability. On the other hand, for S100B ΔCys protein, subsequent Zn^{2+} addition has no effect on folding and it induces a minor destabilization on the protein. Zn^{2+} binding affects the conformation of S100B ΔCys but not the secondary structure of S100B *wt*. It should be also mentioned that the subsequent Cu^{2+} addition to S100B *wt* protein has a minor effect on folding but is highly destabilizing. In the case of S100B ΔCys, Cu^{2+} addtion has the ability to partly restores folding and stability of the protein.

3.4 Zn^{2+} Binding Kinetics

Zn^{2+}-bindig to S100B protein has an important role in terms of conformation and stability. As previously mentioned Cys to Ser mutation does not affect the overall fold. However, helix H_{IV}, where Zn^{2+} binds, becomes truncated and the C-terminal is unstructured. This fact can interfer with Zn^{2+}-binding to S100B and, in particular, can introduce a difference in Zn^{2+} binding kinetics between holo and apo S100B protein.

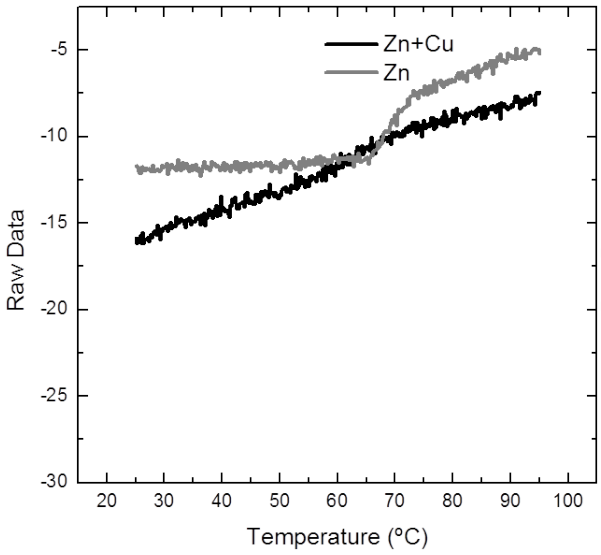

(a) S100B *wt* loaded with Zn^{2+} + later Cu^{2+} addition

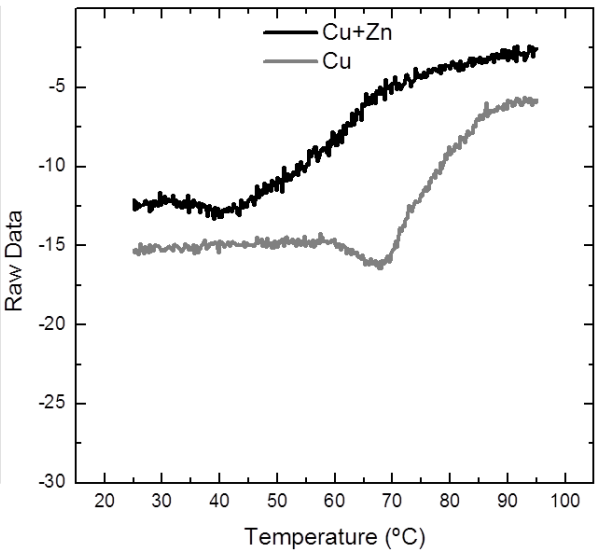

(b) S100B *wt* loaded with Cu^{2+} + later Zn^{2+} addition

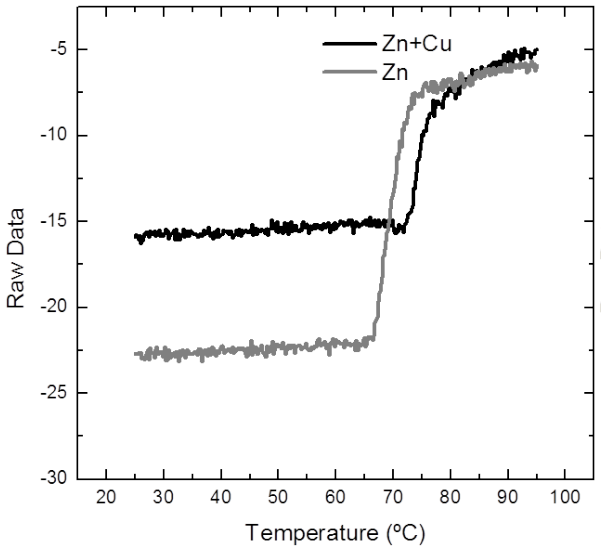

(c) S100B ΔCys loaded with Zn^{2+} + later Cu^{2+} addition

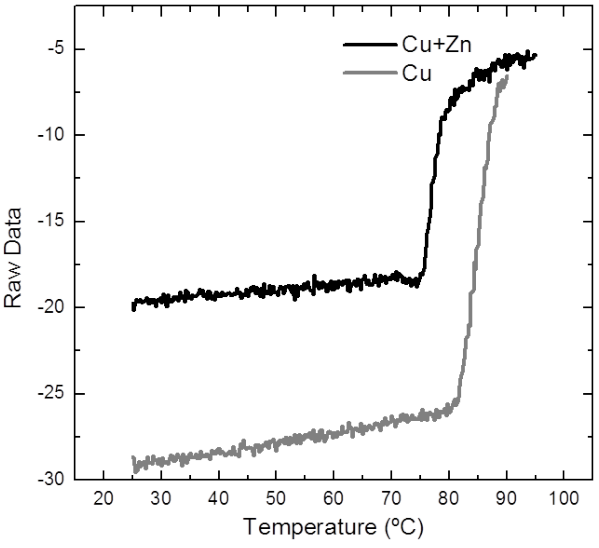

(d) S100B ΔCys loaded with Cu^{2+} + later Zn^{2+} addition

Figure 3.5: Effect of metal binding competition on S100B stability. Representative CD T-Ramps of S100B *wt* and ΔCys loaded with Cu^{2+} and Zn^{2+}.

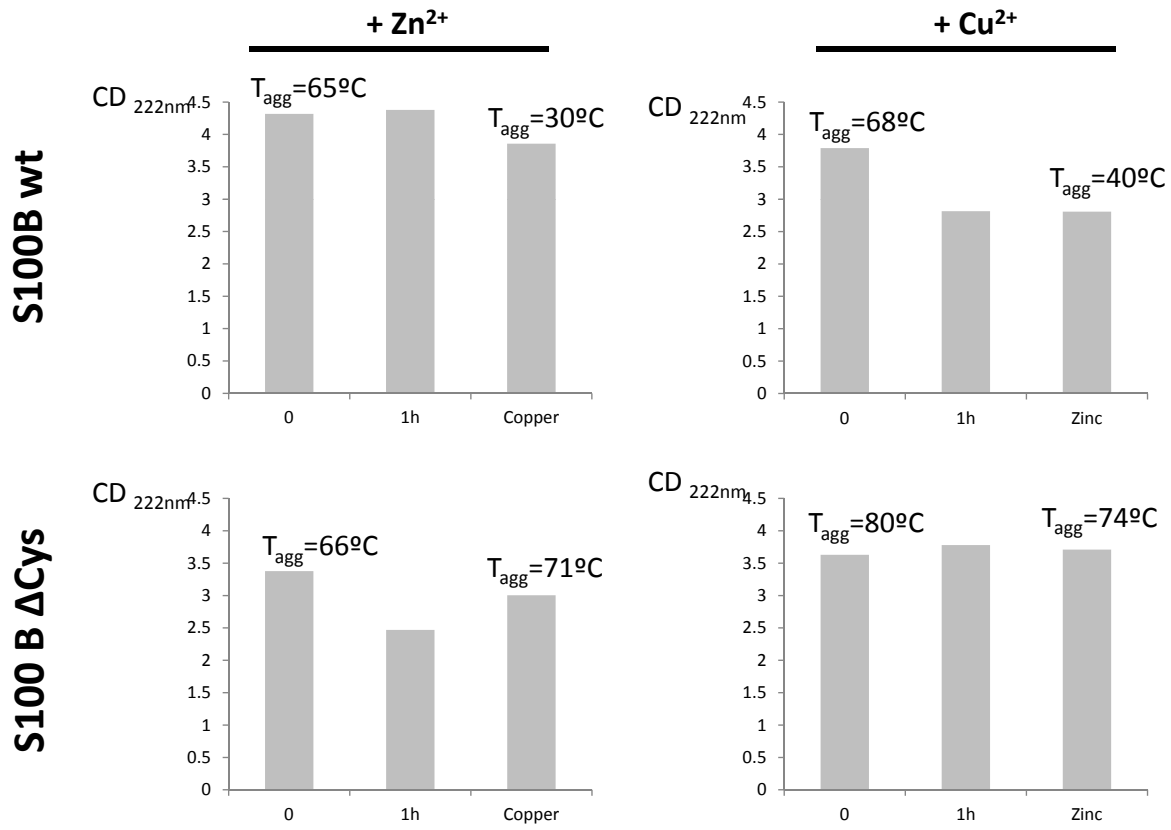

Figure 3.6: Effect of metal binding competition on S100B structure and stability.

In order to study Zn^{2+}-binding to S100B *wt* and ΔCys protein the CD signal of both proteins was followed at 222 nm during 2 h. After an initial CD spectra at 25°C of S100B *wt* apo protein, Zn^{2+} was added. The binding of Zn^{2+} induces an immediate increase in CD signal (**Figure 3.7a**). This fact suggests that Zn^{2+} binding to S100B wt protein occurs immediately after its addition. However, the increase in CD signal at 222 nm is only <5%, which is not significant. On the other hand, the addition of Zn^{2+} to S100B ΔCys apo protein does not induce an immediate response in terms of CD signal (**Figure 3.7b**). This could be explained taking into account the fact that S100B ΔCys protein already have Zn^{2+} and if there is an effect it could not be seen in this sample. In order to better understand the kinetics of Zn^{2+} binding and the difference between S100B wt and ΔCys protein it should be prepared a real apo S100B ΔCys protein.

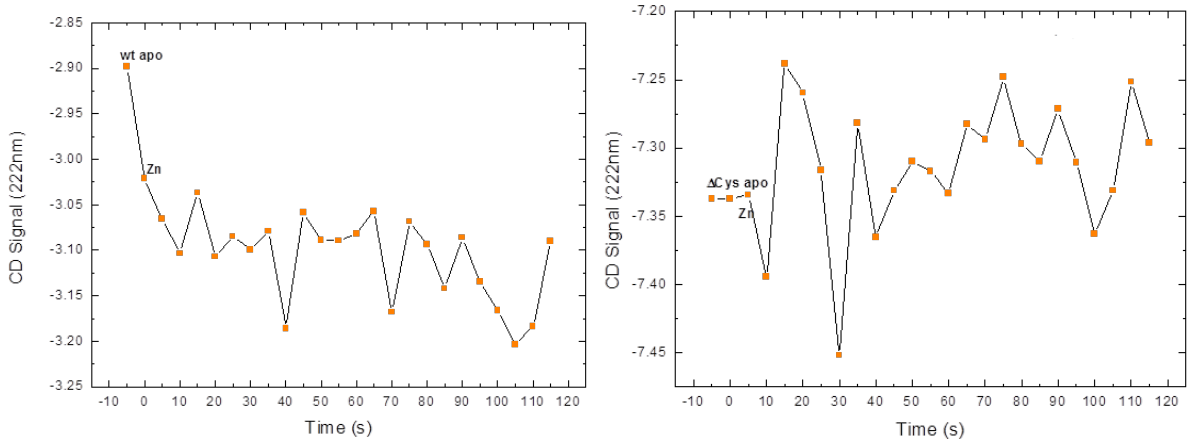

(a) S100B *wt* CD signal at 222 nm **(b)** S100B ΔCys CD signal at 222 nm

Figure 3.7: Zn^{2+}-binding kinetics Representative CD signal at 222 nm of Zn^{2+}-binding to S100B *wt* and ΔCys

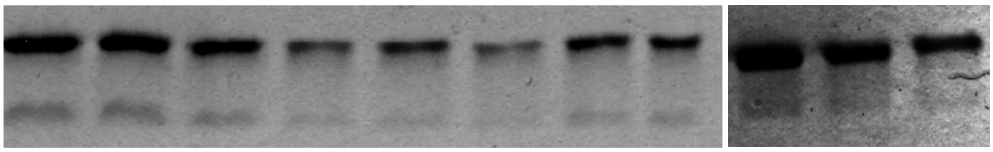

Lane	1	2	3	4	5	6	7	8	9	10	11
Control	+	+	-	-	-	-	-	-	+	-	-
Ca^{2+}	-	-	+	+	-	-	-	-	-	-	-
Zn^{2+}	-	-	-	-	+	+	-	-	-	-	-
Cu^{2+}	-	-	-	-	-	-	-	-	-	+	+
EDTA	-	-	-	-	-	-	+	+	-	-	-
TCEP	-	+	-	+	-	+	-	+	-	-	+

Figure 3.8: Effect of metal binding in cys-dependent dimerization. Native-PAGE for S100B ΔCys protein loaded with Ca^{2+}, Cu^{2+} and Zn^{2+} in the presence of absence of TCEP. Control corresponds to S100B ΔCys apo protein. EDTA is the negative control.

3.5 Effect of metal binding in cys-dependent dimerization

TCEP is a reducing agent capable to protect thiol groups from oxidation by breaking disulfide bonds. S100B has two cys residues so, if not reduced, it can form disulfide

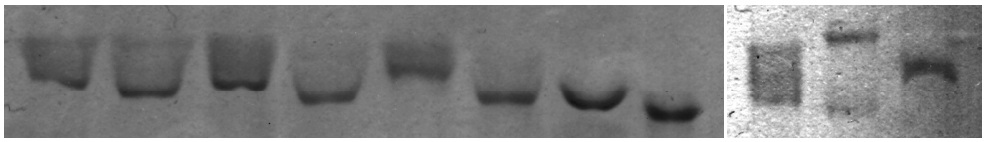

Lane	1	2	3	4	5	6	7	8	9	10	11
Control	+	+	-	-	-	-	-	-	+	-	-
Ca^{2+}	-	-	+	+	-	-	-	-	-	-	-
Zn^{2+}	-	-	-	-	+	+	-	-	-	-	-
Cu^{2+}	-	-	-	-	-	-	-	-	-	+	+
EDTA	-	-	-	-	-	-	+	+	-	-	-
TCEP	-	+	-	+	-	+	-	+	-	-	+

Figure 3.9: Effect of metal binding in cys-dependent dimerization. Native-PAGE for S100B *wt* protein loaded with Ca^{2+}, Cu^{2+} and Zn^{2+} in the presence of absence of TCEP. Control corresponds to S100B wt apo protein. EDTA is the negative control.

bonds with other subunits or proteins. In order to study the role of metal binding in cys-dependent dimerization of S100B protein the effect of TCEP was studied. As it was expected, the presence of TCEP does not affect the migration of S100B ΔCys in the gels. In fact, all metal-loaded samples present the same pattern in a native gel (**Figure 3.8**). On the other hand, for S100B wt protein, it can be observed a different behaviour (**Figure 3.9**). In this case, the samples with and without TCEP migrate in a different pattern. The effect of TCEP addition is the same for all protein samples except for S100B wt loaded with Cu^{2+} (**Figure 3.9**). Cu^{2+} binding showed two distinct bands, the more intense with a higher molecular mass, when compared with the other metal loaded samples. S100B wt protein loaded with Cu^{2+} and in the presence of TCEP presents only one band.

S100B protein incubated with Ca^{2+}, Cu^{2+} and Zn^{2+} and in the presence or abscense TCEP was analyzed by SDS-PAGE under non-reducing conditions. All samples a band near 6.5 kDa (monomer) except S100B wt protein loaded with Cu^{2+} that has a molecular mass of 23 kDa (**Figure 3.10**).

It has been reported that cys residues are not necessary for the noncovalent dimerization of S100B [**154**]. Although S100B exists as a noncovalent dimer in solution this disulfide-linked dimer only occurs in the presence of Cu^{2+}, suggesting that only Cu^{2+} (and not Zn^{2+} or Ca^{2+}) has an important role in disulfide bond formation between S100B subunits.

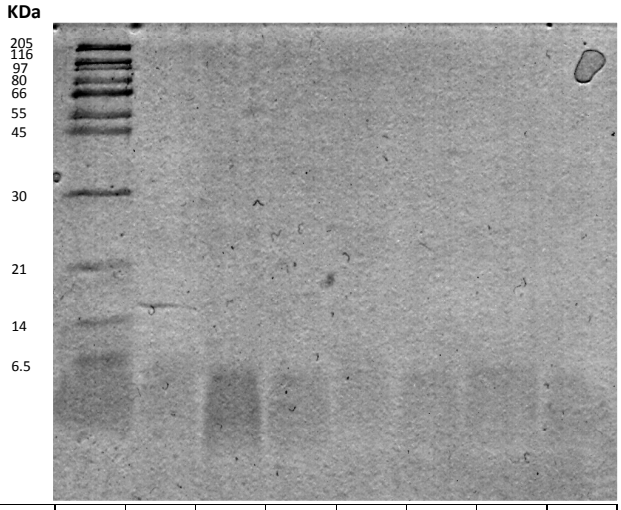

Lane	1	2	3	4	5	6	7	8
	MW							
Control Δ Cys		+	-	-	-	-	-	-
Control wt		-	+	+	-	-	-	-
wt + Ca $^{2+}$		-	-	-	+	+	-	-
wt + EDTA		-	-	-	-	-	+	+
TCEP		-	-	+	-	+	-	+

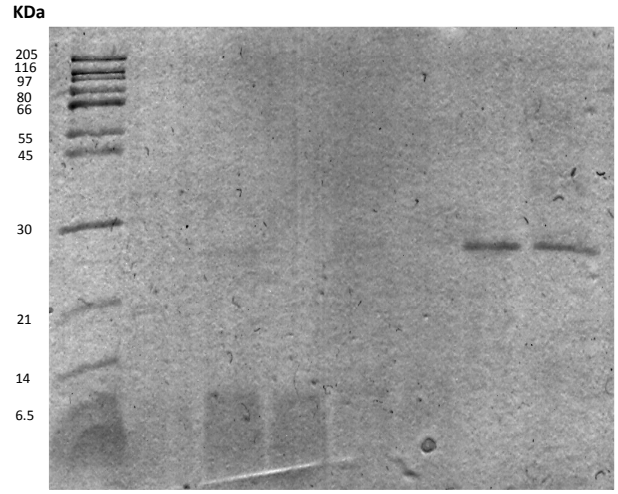

Lane	1	2	3	4	5	6	7	8
	MW							
Control Δ Cys		+	-	-	-	-	-	-
Control wt		-	+	+	-	-	-	-
wt + Zn $^{2+}$		-	-	-	+	+	-	-
wt + Cu $^{2+}$		-	-	-	-	-	+	+
TCEP		-	-	+	-	+	-	+

Figure 3.10: Effect of metal binding in cys-dependent dimerization. SDS-PAGE for S100B *wt* protein loaded with Ca^{2+}, Cu^{2+} and Zn^{2+}. Control wt is S100B wt apo protein. Control ΔCys is S100B ΔCys apo protein. EDTA is the negative control.

These results are in agreement with Lee and coworkers [**155**] that described the copper-dependent formation of disulfide-linked dimer of S100B.

Chapter 4

Concluding Remarks

S100B is the most abundant soluble protein in the human brain, being highly expressed in astrocytes. Besides Ca^{2+} it has also the ability to bind Cu^{2+} and Zn^{2+}. These metals are present in the synaptic space at high levels and are involved in several neurodegenerative disorders, including AD [**139**]. S100B protein is involved in several pathological processes in which metal homeostasis is imbalanced leading to a modified protein function. In fact, AD has been the most extensively studied neurodegenerative disease regarding S100B pathology. Moreover, it is well known that metal ions, and in particular Cu^{2+} and Zn^{2+}, are also involved in the disease playing an important role on its development. These metal ions have also an important role in the regulation and, therefore, in the function of S100B protein. However, their consequences on protein conformation and stability are not characterized.

This work extensively address the effects of metal binding on the folding and stability of S100B protein. With this purpose we have studied the wild type form of human S100B as well as Cys-to-Ser mutated variant, S100B ΔCys. The structural changes induced by metal ions in S100B and the thermal stability of the protein were studied using far-UV circular dichroism (CD). The CD spectra of S100B wt protein in the apo and holo state suggest that not only different metals induce different conformational changes but also that these changes are different depending on the protein (wt or ΔCys). Moreover, the stability of the protein monitored by thermal denaturation is quite different in distinct metal loaded samples.

S100B protein undergo substantial conformational and thermal stability changes upon Zn^{2+} and Cu^{2+}-binding. Unlike Ca^{2+}, these two metal ions are responsible for destabiliz-

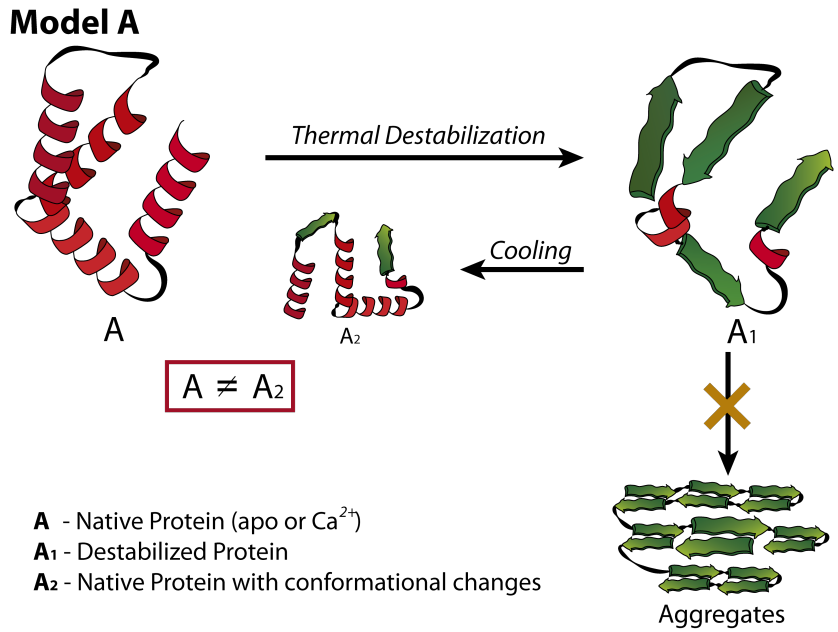

(a) S100B apo or Ca^{2+}-loaded

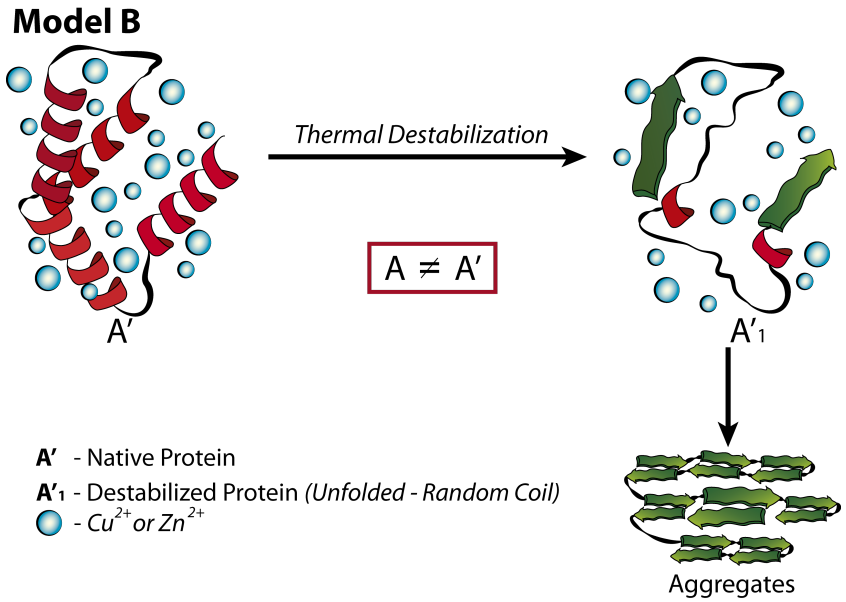

(b) S100B Cu^{2+} or Zn^{2+}-loaded

Figure 4.1: Model of S100B thermal denaturation mechanisms upon metal binding.

ing the protein leading to aggregation. On the other hand, S100B apo and Ca^{2+}-loaded protein do not aggregate. However, these two samples suffer a conformational change after thermal denaturation. In fact, a part of the α-helix secondary structure content is lost and it is visible the appereance of new β-sheet structural elements. These effects were observed for both S100B proteins and are represented in **Figure 4.1a** and **Figure 4.1b**, a model that we build up taking into account the results obtained for conformational and thermal stability of S100B wt protein upon metal ion binding. The study of Cu^{2+} and Zn^{2+} binding competition revealed that Cu^{2+} has the ability to displace Zn^{2+} from the binding site distabilizing S100B wt protein ($\Delta T_{agg} = 35°C$). However, for S100B ΔCys, although Cu^{2+} also displaces Zn^{2+}, it has the opposite effect, stabilizing the mutated protein ($\Delta T_{agg} = -5°C$) However, for all of these samples protein aggregation was observed. **Figure 4.2** and **Figure 4.3** are two models that exemplify the mechanisms described above. We also observed that Cu^{2+}, but not Zn^{2+} or Ca^{2+}, has the ability to promote intermolecular disulfide bond formation between S100B subunits.

All together, these results led us to hypothesize that metal induced conformational changes may account for the buildup of conformers that have increased oligomerization propensity and that this may play a role in S100B function and on its interactors. This possibility is particularly relevant considering the interplay of S100B with amyloid-β peptide, which are suggestive of an even more interesting engagement in AD.

The experimental studies presented here brought a valid contribution to clarify the mechanisms underlying metal ion modulation of S100B conformation and stability. However, many questions remain unanswered. So, in order to understand the interaction of metal ions with this cytokine should be carried out other experiments. Monitoring thermal denaturation using Dynamic Light Scattering would be an important contribute to better understand S100B aggregation modulated by metal binding. Moreover, it could provide an overview of the S100B oligomeric species formed upon metal binding. Chemical denaturation could also be usefull to better characterize S100B stability and to determine thermodynamic parameters. In order to realize the role of cysteines in fibrillation kinetics of S100B protein ThT fluorescence assays would be helpful. The interaction between S100B, A-β and RAGE should also be studied in order to establish the possible involvement of S100B protein in synaptic protein aggregation in neurodegeneration, in particular on AD.

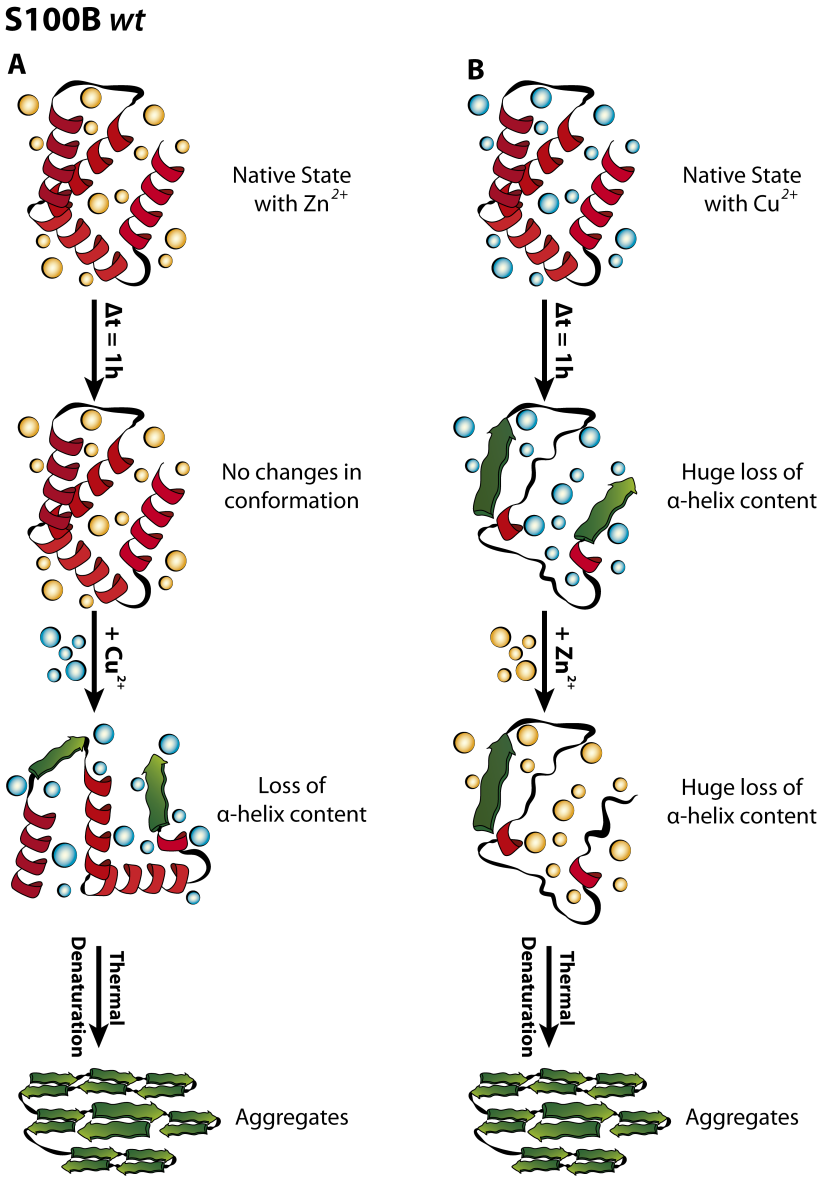

Figure 4.2: Model of S100B wt metal binding competition between Cu^{2+} and Zn^{2+}.

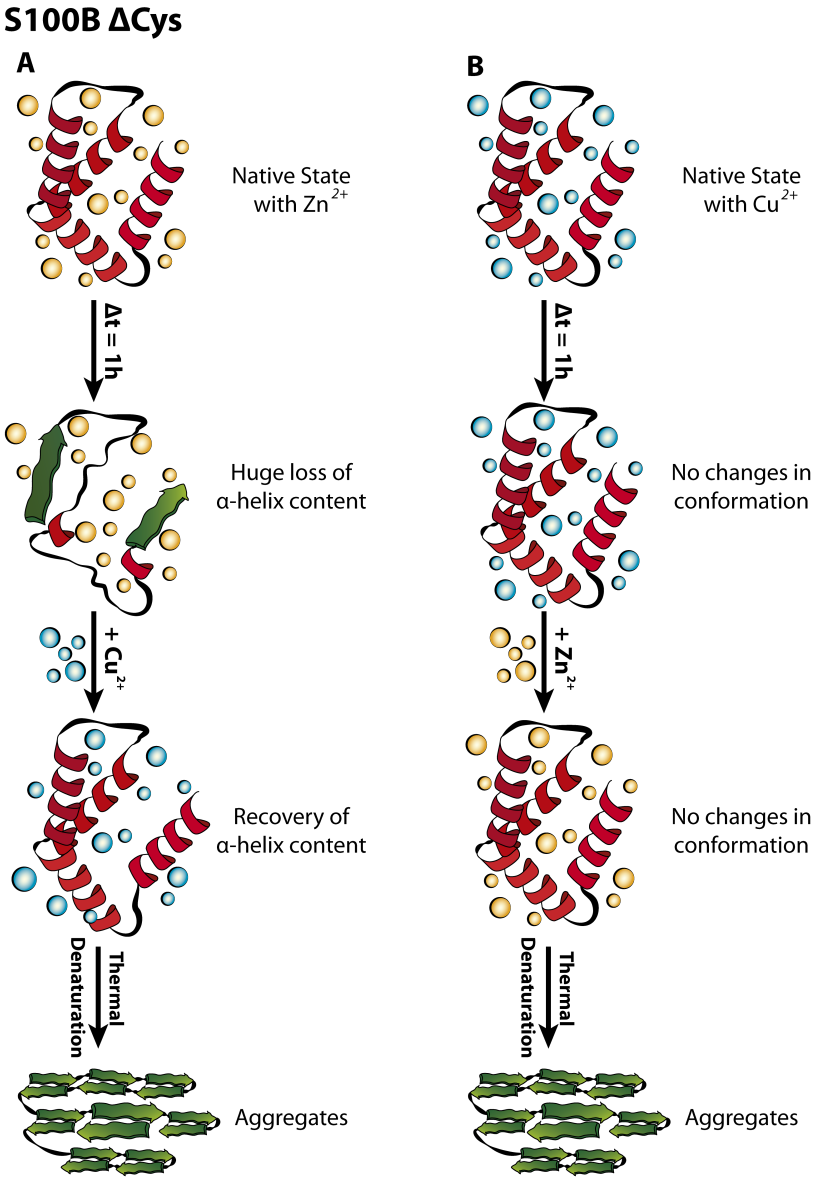

Figure 4.3: Model of S100B ΔCys metal binding competition between Cu^{2+} and Zn^{2+}.

Bibliography

[1] CM Gomes and P Wittung-Stafshede. *Protein Folding and Metal Ions: Mechanisms, Biology and Disease*. CRC Press Group. Taylor & Francis (USA), 2010.

[2] C Andreini, I Bertini, G Cavallaro, GL Holliday, and JM Thornton. Metal ions in biological catalysis: from enzyme databases to general principles. *Journal Of Biological Inorganic Chemistry*, 13:1205–1218, 2008.

[3] E Permyakov. *Metalloproteomics*, volume 2. Wiley-Interscience, 2009.

[4] DE Fenton. *Biocoordination chemistry*. Oxford university press, 1995.

[5] MR Bleackley and TA MacGillivray. Transition metal homeostasis: from yeast to human disease. *Biometals*, pages 1–25, 2011.

[6] HM Botelho. *Metal Ions and Protein Folding: Conformationl and Functional Interplay*. PhD thesis, Instituto de Tecnologia Química e Biológica, Universidade Nova de Lisboa, Lisboa, 2010.

[7] M Valko, H Morris, and MTD Cronin. Metals, toxicity and oxidative stress. *Current Medicinal Chemistry*, 12:1161–1208, 2005.

[8] KJ Waldron, JC Rutherford, D Ford, and NJ Robinson. Metalloproteins and metal sensing. *Nature*, 460:823–830, 2009.

[9] FP Guengerich. Thematic minireview series: Metals in biology 2010. *Journal of Biological Chemistry*, 285:26727, 2010.

[10] GA Petsko and D Ringe. *Protein structure and function*. Sinauer Associates Inc, 2004.

[11] C.B. Anfinsen et al. Principles that govern the folding of protein chains. *Science*, 181:223–230, 1973.

[12] C Levinthal. Mossbauer spectroscopy in biological systems. In *Proceedings of a meeting held at Allerton House. P Debrunner, JCM Tsibris, and E Munck, editors. University of Illinois Press, Urbana, IL*, 1969.

[13] KA Dill and HS Chan. From levinthal to pathways to funnels. *Nature Structural Biology*, 4:10–19, 1997.

[14] BJ Henriques. *Defective Protein Folding and Function in Metabolic Disorders: Studies on the Mitochondrial Flavoenzyme ETF*. PhD thesis, Instituto de Tecnologia Química e Biológica, Universidade Nova de Lisboa, Lisboa, 2010.

[15] J M Sanchez-Ruiz. Protein kinetic stability. *Biophys Chem*, 148:1, 2010.

[16] CN Pace. Energetics of protein hydrogen bonds. *Nature Structural & Molecular Biology*, 16:681–682, 2009.

[17] C K Mathews, K E van Holde, and K G Ahern. *Biochemistry*. Cummings, Redwood City, CA, 1990.

[18] D Whitford. *Proteins: structure and function*. Wiley, 2005.

[19] A M Lesk. *Introduction to protein science: architecture, function and genomics*. Oxford University Press, USA, 2004.

[20] JW Yewdell. Serendipity strikes twice: the discovery and rediscovery of defective ribosomal products (drips). *Cellular and molecular biology (Noisy-le-Grand, France)*, 51:635, 2005.

[21] N Gregersen, P Bross, S Vang, and JH Christensen. Protein misfolding and human disease. *Annu. Rev. Genomics Hum. Genet.*, 7:103–124, 2006.

[22] F Chiti and CM Dobson. Protein misfolding, functional amyloid, and human disease. *Annual review of biochemistry*, 75:333, 2006.

[23] K Blennow, MJ de Leon, and H Zetterberg. Alzheimer's disease. *Lancet*, 368:387–403, 2006.

[24] VN Uversky and D Eliezer. Biophysics of parkinsons disease: Structure and aggregation of-synuclein. *Current Protein and Peptide Science*, 10:483–499, 2009.

[25] BS Shastry. Neurodegenerative disorders of protein aggregation. *Neurochemistry international*, 43:1–7, 2003.

[26] I Bertini, A Sigel, and H Sigel. *Handbook on metalloproteins*. CRC, 2001.

[27] W L DeLano. The PyMOL molecular graphics system, 2002.

[28] HB Gray. Biological inorganic chemistry at the beginning of the 21st century. *Proceedings of the National Academy of Sciences*, 100:3563, 2003.

[29] FA Tezcan, WM Findley, BR Crane, SA Ross, JG Lyubovitsky, HB Gray, and JR Winkler. Using deeply trapped intermediates to map the cytochrome c folding landscape. *Proceedings of the National Academy of Sciences*, 99:8626–8630, 2002.

[30] JG Lyubovitsky, HB Gray, and JR Winkler. Mapping the cytochrome c folding landscape. *Journal of the American Chemical Society*, 124:5481–5485, 2002.

[31] WR Fisher, H Taniuchi, and CB Anfinsen. On the role of heme in the formation of the structure of cytochrome c. *Journal of Biological Chemistry*, 248:3188–3195, 1973.

[32] M Yamanaka, H Mita, Y Yamamoto, and Y Sambongi. Heme is not required for aquifex aeolicus cytochrome c (555) polypeptide folding. *Bioscience, biotechnology, and biochemistry*, 73:2022–2025, 2009.

[33] A Borgia, S Gianni, M Brunori, and C Travaglini-Allocatelli. Fast folding kinetics and stabilization of apo-cytochrome c. *FEBS letters*, 582:1003–1007, 2008.

[34] LN Lin, AB Mason, RC Woodworth, and JF Brandts. Calorimetric studies of the n-terminal half-molecule of transferrin and mutant forms modified near the fe (3+)-binding site. *Biochemical Journal*, 293:517–522, 1993.

[35] CE Outten et al. Femtomolar sensitivity of metalloregulatory proteins controlling zinc homeostasis. *Science*, 292:2488, 2001.

[36] H Tapiero and KD Tew. Trace elements in human physiology and pathology: zinc and metallothioneins. *Biomedecine & Pharmacotherapy*, 57:399–411, 2003.

[37] KA McCall, C Huang, and CA Fierke. Function and mechanism of zinc metalloenzymes. *The Journal of nutrition*, 130:1437S–1466S, 2000.

[38] C Andreini, L Banci, I Bertini, and A Rosato. Counting the zinc-proteins encoded in the human genome. *Journal of proteome research*, 5:196–201, 2006.

[39] ES Lander, LM Linton, B Birren, C Nusbaum, MC Zody, J Baldwin, K Devon, K Dewar, M Doyle, W FitzHugh, et al. Initial sequencing and analysis of the human genome. *Nature*, 409:860–921, 2001.

[40] AD Frankel, JM Berg, and CO Pabo. Metal-dependent folding of a single zinc finger from transcription factor iiia. *Proceedings of the National Academy of Sciences*, 84:4841–4845, 1987.

[41] SZ Potter, H Zhu, BF Shaw, JA Rodriguez, PA Doucette, SH Sohn, A Durazo, KF Faull, EB Gralla, AM Nersissian, et al. Binding of a single zinc ion to one subunit of copper-zinc superoxide dismutase apoprotein substantially influences the structure and stability of the entire homodimeric protein. *Journal of the American Chemical Society*, 129:4575–4583, 2007.

[42] Y Yang and HM Zhou. Effect of zinc ions on conformational stability of yeast alcohol dehydrogenase. *Biochemistry (Moscow)*, 66(1):47–54, 2001.

[43] WP Le, SX Yan, YX Zhang, and HM Zhou. Acid-induced folding of yeast alcohol dehydrogenase under low ph conditions. *Journal of biochemistry*, 119:674, 1996.

[44] WP Le, SX Yan, S Li, HN Zhong, and HM Zhou. Alkaline unfolding and salt-induced folding of yeast alcohol dehydrogenase under high ph conditions. *International Journal of Peptide and Protein Research*, 47(6):484–490, 1996.

[45] CJ Lin, HC Huang, and ZF Jiang. Cu (ii) interaction with amyloid-β peptide: A review of neuroactive mechanisms in ad brains. *Brain research bulletin*, 82:235–242, 2010.

[46] P Wittung-Stafshede. Role of cofactors in protein folding. *Accounts of chemical research*, 35:201–208, 2002.

[47] CJ Wilson, D Apiyo, and P Wittung-Stafshede. Role of cofactors in metalloprotein folding. *Quarterly Reviews of Biophysics*, 37:285–314, 2004.

[48] V De Filippis, VB Vassiliev, M Beltramini, A Fontana, B Salvato, and VS Gaitskhoki. Evidence for the molten globule state of human apo-ceruloplasmin. *Biochimica et Biophysica Acta (BBA)-Protein Structure and Molecular Enzymology*, 1297:119–123, 1996.

[49] L Santamaria-Kisiel, AC Rintala-Dempsey, and GS Shaw. Calcium-dependent and-independent interactions of the s100 protein family. *Biochemical Journal*, 396:201–214, 2006.

[50] BW Schafer and CW Heizmann. The s100 family of ef-hand calcium-binding proteins: functions and pathology. *Trends in biochemical sciences*, 21:134–140, 1996.

[51] EA Permyakov, AV Ostrovsky, EA Burstein, PG Pleshanov, and C Gerday. Parvalbumin conformers revealed by steady-state and time-resolved fluorescence spectroscopy. *Archives of biochemistry and biophysics*, 240:781–791, 1985.

[52] M Laberge, WW Wright, K Sudhakar, PA Liebman, and JM Vanderkooi. Conformational effects of calcium release from parvalbumin: comparison of computational simulations with spectroscopic investigations. *Biochemistry*, 36:5363–5371, 1997.

[53] V Forge, RT Wijesinha, J Balbach, K Brew, CV Robinson, C Redfield, and CM Dobson. Rapid collapse and slow structural reorganisation during the refolding of bovine [alpha]-lactalbumin1. *Journal of molecular biology*, 288:673–688, 1999.

[54] M Ikeguchi, K Kuwajima, and S Sugai. Ca2+-induced alteration in the unfolding behavior of alpha-lactalbumin. *Journal of biochemistry*, 99:1191, 1986.

[55] NA Bushmarina, CE Blanchet, G Vernier, and V Forge. Cofactor effects on the protein folding reaction: Acceleration of α-lactalbumin refolding by metal ions. *Protein science*, 15:659–671, 2006.

[56] KR Rao and K Brew. Calcium regulates folding and disulfide-bond formation in [alpha]-lactalbumin. *Biochemical and Biophysical Research Communications*, 163:1390–1396, 1989.

[57] BW Moore. A soluble protein characteristic of the nervous system. *Biochemical and biophysical research communications*, 19:739, 1965.

[58] G Fritz, HM Botelho, LA Morozova-Roche, and CM Gomes. Natural and amyloid self-assembly of s100 proteins: structural basis of functional diversity. *FEBS Journal*, 277:4578–4590, 2010.

[59] G Fritz and CW Heizmann. *Handbook of Metalloproteins*. John Wiley & Sons, Chichester, UK, 2004.

[60] D Engelkamp, BW Schäfer, MG Mattei, P Erne, and CW Heizmann. Six s100 genes are clustered on human chromosome 1q21: identification of two genes coding for the two previously unreported calcium-binding proteins s100d and s100e. *Proceedings of the National Academy of Sciences*, 90:6547–6551, 1993.

[61] BW Schäfer, R Wicki, D Engelkamp, MG Mattei, and CW Heizmann. Isolation of a yac clone covering a cluster of nine s100 genes on human chromosome 1q21: rationale for a new nomenclature of the s100 calcium-binding protein family. *Genomics*, 25:638–643, 1995.

[62] I Marenholz, CW Heizmann, and G Fritz. S100 proteins in mouse and man: from evolution to function and pathology (including an update of the nomenclature). *Biochemical and biophysical research communications*, 322:1111–1122, 2004.

[63] I Salama, PS Malone, F Mihaimeed, and JL Jones. A review of the s100 proteins in cancer. *European Journal of Surgical Oncology (EJSO)*, 34:357–364, 2008.

[64] RE Mrak and WST Griffin. The role of activated astrocytes and of the neurotrophic cytokine s100b in the pathogenesis of alzheimer's disease. *Neurobiology of aging*, 22:915–922, 2001.

[65] P Björk, A Björk, T Vogl, M Stenström, D Liberg, A Olsson, J Roth, F Ivars, and T Leanderson. Identification of human s100a9 as a novel target for treatment of autoimmune disease via binding to quinoline-3-carboxamides. *PLoS biology*, 7:e97, 2009.

[66] E Leclerc, G Fritz, SW Vetter, and CW Heizmann. Binding of s100 proteins to rage: an update. *Biochimica et Biophysica Acta (BBA)-Molecular Cell Research*, 1793:993–1007, 2009.

[67] T Ostendorp, E Leclerc, A Galichet, M Koch, N Demling, B Weigle, CW Heizmann, PMH Kroneck, and G Fritz. Structural and functional insights into rage activation by multimeric s100b. *The EMBO Journal*, 26:3868–3878, 2007.

[68] R Donato. Rage: a single receptor for several ligands and different cellular responses: the case of certain s100 proteins. *Current Molecular Medicine*, 7:711–724, 2007.

[69] T Vogl, K Tenbrock, S Ludwig, N Leukert, C Ehrhardt, MA Van Zoelen, W Nacken, D Foell, T Van der Poll, C Sorg, et al. Mrp8 and mrp14 are endogenous activators of toll-like receptor 4, promoting lethal, endotoxin-induced shock. *Nature medicine*, 13:1042–1049, 2007.

[70] NM Marlatt, BL Boys, L Konermann, and GS Shaw. Formation of monomeric s100b and s100a11 proteins at low ionic strength. *Biochemistry*, 48:1954–1963, 2009.

[71] RH Kretsinger and CE Nockolds. Carp muscle calcium-binding protein. *Journal of Biological chemistry*, 248:3313, 1973.

[72] CW Heizmann T Ostendorp, J Diez and G Fritz. The crystal structures of human s100b in the zinc- and calcium-loaded state at three ph values reveal zinc ligand swapping. *Biochimica et Biophysica Acta (BBA)-Molecular Cell Research*, 1813:1083–1091, 2011.

[73] LR Otterbein, J Kordowska, C Witte-Hoffmann, CL Wang, and R Dominguez. Crystal structures of s100a6 in the Ca^{2+}-free and Ca^{2+}-bound states:: The calcium sensor mechanism of s100 proteins revealed at atomic resolution. *Structure*, 10:557–567, 2002.

[74] A Lewit-Bentley and S Réty. Ef-hand calcium-binding proteins. *Current Opinion in Structural Biology*, 10:637–643, 2000.

[75] S Henikoff, EA Greene, S Pietrokovski, P Bork, TK Attwood, and L Hood. Gene families: the taxonomy of protein paralogs and chimeras. *Science*, 278:609–614, 1997.

[76] F Capozzi, F Casadei, and C Luchinat. Ef-hand protein dynamics and evolution of calcium signal transduction: an nmr view. *Journal of Biological Inorganic Chemistry*, 11:949–962, 2006.

[77] CW Heizmann and JA Cox. New perspectives on s100 proteins: a multi-functional Ca^{2+} Zn^{2+}- and Cu^{2+}-binding protein family. *Biometals*, 11:383–397, 1998.

[78] A Mandinova, D Atar, BW Schafer, M Spiess, U Aebi, and CW Heizmann. Distinct subcellular localization of calcium binding s100 proteins in human smooth muscle cells and their relocation in response to rises in intracellular calcium. *Journal of Cell Science*, 111:2043–2054, 1998.

[79] M Koch, S Bhattacharya, T Kehl, M Gimona, M Vasak, W Chazin, CW Heizmann, PMH Kroneck, and G Fritz. Implications on zinc binding to s100a2. *Biochimica et Biophysica Acta (BBA)-Molecular Cell Research*, 1773:457–470, 2007.

[80] OV Moroz, EV Blagova, AJ Wilkinson, KS Wilson, and IB Bronstein. The crystal structures of human s100a12 in apo form and in complex with zinc: new insights into s100a12 oligomerisation. *Journal of molecular biology*, 391:536–551, 2009.

[81] DE Brodersen, J Nyborg, and M Kjeldgaard. Zinc-binding site of an s100 protein revealed. two crystal structures of Ca^{2+}-bound human psoriasin (s100a7) in the Zn^{2+}-loaded and Zn^{2+}-free states. *Biochemistry*, 38:1695–1704, 1999.

[82] TH Charpentier, PT Wilder, MA Liriano, KM Varney, E Pozharski, AD MacKerell Jr, A Coop, EA Toth, and DJ Weber. Divalent metal ion complexes of s100b in the absence and presence of pentamidine. *Journal of molecular biology*, 382:56–73, 2008.

[83] BW Schäfer, JM Fritschy, P Murmann, H Troxler, I Durussel, CW Heizmann, and JA Cox. Brain s100a5 is a novel calcium-, zinc-, and copper ion-binding protein of the ef-hand superfamily. *Journal of Biological Chemistry*, 275:30623–30630, 2000.

[84] OV Moroz, AA Antson, SJ Grist, NJ Maitland, GG Dodson, KS Wilson, E Lukanidin, and IB Bronstein. Structure of the human s100a12-copper complex: implications for host-parasite defence. *Acta Crystallographica Section D: Biological Crystallography*, 59:859–867, 2003.

[85] M Landriscina, C Bagalá, A Mandinova, R Soldi, I Micucci, S Bellum, I Prudovsky, and T Maciag. Copper induces the assembly of a multiprotein aggregate implicated in the release of fibroblast growth factor 1 in response to stress. *Journal of Biological Chemistry*, 276:25549, 2001.

[86] T Nishikawa, ISM Lee, N Shiraishi, T Ishikawa, Y Ohta, and M Nishikimi. Identification of s100b protein as copper-binding protein and its suppression of copper-induced cell damage. *Journal of Biological Chemistry*, 272:23037, 1997.

[87] V Sivaraja, TK Kumar, D Rajalingam, I Graziani, I Prudovsky, and C Yu. Copper binding affinity of s100a13, a key component of the fgf-1 nonclassical copper-dependent release complex. *Biophysical journal*, 91:1832–1843, 2006.

[88] DB Zimmer, J Chaplin, A Baldwin, and M Rast. S100-mediated signal transduction in the nervous system and neurological diseases. *Cellular and molecular biology (Noisy-le-Grand, France)*, 51:201, 2005.

[89] RE Mrak and W. Griffin. Trisomy 21 and the brain. *Journal of Neuropathology & Experimental Neurology*, 63:679, 2004.

[90] LJ Van Eldik and MS Wainwright. The janus face of glial-derived s100b: beneficial and detrimental functions in the brain. *Restorative neurology and neuroscience*, 21:97–108, 2003.

[91] AC Drohat, JC Amburgey, F Abildgaard, MR Starich, D Baldisseri, and DJ Weber. Solution structure of rat apo-s100b ($\beta\beta$) as determined by nmr spectroscopy. *Biochemistry*, 35:11577–11588, 1996.

[92] PM Kilby, LJ Van Eldik, and GC Roberts. The solution structure of the bovine s100b protein dimer in the calcium-free state. *Structure*, 4:1041–1052, 1996.

[93] AC Drohat, DM Baldisseri, RR Rustandi, and DJ Weber. Solution structure of calcium-bound rat s100b ($\beta\beta$) as determined by nuclear magnetic resonance spectroscopy. *Biochemistry*, 37:2729–2740, 1998.

[94] H Matsumura, T Shiba, T Inoue, S Harada, and Y Kai. A novel mode of target recognition suggested by the 2.0 å structure of holo s100b from bovine brain. *Structure*, 6:233–241, 1998.

[95] SP Smith and GS Shaw. A novel calcium-sensitive switch revealed by the structure of human s100b in the calcium-bound form. *Structure*, 6:211–222, 1998.

[96] PT Wilder, KM Varney, MB Weiss, RK Gitti, and DJ Weber. Solution structure of zinc- and calcium-bound rat s100b as determined by nuclear magnetic resonance spectroscopy. *Biochemistry*, 44:5690–5702, 2005.

[97] RR Rustandi, DM Baldisseri, and DJ Weber. Structure of the negative regulatory domain of p53 bound to s100b ($\beta\beta$). *Nature Structural & Molecular Biology*, 7:570–574, 2000.

[98] S Bhattacharya, E Large, CW Heizmann, BA Hemmings, and WJ Chazin. Structure of the ca2+/s100b/ndr kinase peptide complex: insights into s100 target specificity and activation of the kinase. *Biochemistry*, 42:14416–14426, 2003.

[99] KG Inman, R Yang, RR Rustandi, KE Miller, DM Baldisseri, and DJ Weber. Solution nmr structure of s100b bound to the high-affinity target peptide trtk-12. *Journal of molecular biology*, 324:1003–1014, 2002.

[100] AC Drohat, E Nenortas, D Beckett, and DJ Weber. Oligomerization state of s100b at nanomolar concentration determined by large-zone analytical gel filtration chromatography. *Protein science*, 6:1577–1582, 1997.

[101] R Donato. Intracellular and extracellular roles of s100 proteins. *Microscopy research and technique*, 60:540–551, 2003.

[102] CW Heizmann, G Fritz, BW Schafer, et al. S100 proteins: structure, functions and pathology. *Front Biosci*, 7:1356–1368, 2002.

[103] J Baudier and D Gerard. Ions binding to s100 proteins. ii. conformational studies and calcium-induced conformational changes in s100 alpha alpha protein: the effect of acidic ph and calcium incubation on subunit exchange in s100a (alpha beta) protein. *Journal of Biological Chemistry*, 261:8204–8212, 1986.

[104] E Leclerc, E Sturchler, and SW Vetter. The s100b/rage axis in alzheimer's disease. *Cardiovascular Psychiatry and Neurology*, 2010.

[105] R Donato, G Sorci, F Riuzzi, C Arcuri, R Bianchi, F Brozzi, C Tubaro, and I Giambanco. S100b's double life: Intracellular regulator and extracellular signal. *Biochimica et Biophysica Acta (BBA)-Molecular Cell Research*, 1793:1008–1022, 2009.

[106] GE Davey, P Murmann, and CW Heizmann. Intracellular Ca^{2+} and Zn^{2+} levels regulate the alternative cell density-dependent secretion of s100b in human glioblastoma cells. *Journal of Biological Chemistry*, 276:30819, 2001.

[107] MA Hofmann, S Drury, C Fu, W Qu, A Taguchi, Y Lu, C Avila, N Kambham, A Bierhaus, P Nawroth, et al. Rage mediates a novel proinflammatory axis: A central cell surface receptor for s100/calgranulin polypeptides. *Cell*, 97:889–901, 1999.

[108] J Hu, F Castets, JL Guevara, and LJ Van Eldik. S100β stimulates inducible nitric oxide synthase activity and mrna levels in rat cortical astrocytes. *Journal of Biological Chemistry*, 271:2543, 1996.

[109] R Donato. S100: a multigenic family of calcium-modulated proteins of the ef-hand type with intracellular and extracellular functional roles. *The international journal of biochemistry & cell biology*, 33:637–668, 2001.

[110] J Hu, A Ferreira, and LJ Van Eldik. S100β induces neuronal cell death through nitric oxide release from astrocytes. *Journal of neurochemistry*, 69:2294–2301, 1997.

[111] T Koppal, AG Lam, L Guo, and LJ Van Eldik. S100b proteins that lack one or both cysteine residues can induce inflammatory responses in astrocytes and microglia. *Neurochemistry international*, 39:401–407, 2001.

[112] G Sorci, R Bianchi, F Riuzzi, C Tubaro, C Arcuri, I Giambanco, and R Donato. S100b protein, a damage-associated molecular pattern protein in the brain and heart, and beyond. *Cardiovascular psychiatry and neurology*, 2010, 2010.

[113] T Mori, N Koyama, GW Arendash, Y Horikoshi-Sakuraba, J Tan, and T Town. Overexpression of human s100b exacerbates cerebral amyloidosis and gliosis in the tg2576 mouse model of alzheimer's disease. *Glia*, 58:300–314, 2010.

[114] RH Selinfreund, SW Barger, WJ Pledger, and LJ Van Eldik. Neurotrophic protein s100 beta stimulates glial cell proliferation. *Proceedings of the National Academy of Sciences*, 88:3554–3558, 1991.

[115] HJ Huttunen, J Kuja-Panula, G Sorci, AL Agneletti, R Donato, and H Rauvala. Coregulation of neurite outgrowth and cell survival by amphoterin and s100 proteins through receptor for advanced glycation end products (rage) activation. *Journal of Biological Chemistry*, 275:40096–40105, 2000.

[116] MR Fernandez-Fernandez, DB Veprintsev, and AR Fersht. Proteins of the s100 family regulate the oligomerization of p53 tumor suppressor. *Proceedings of the National Academy of Sciences*, 102:4735–4740, 2005.

[117] J Baudier, C Delphin, D Grunwald, S Khochbin, and JJ Lawrence. Characterization of the tumor suppressor protein p53 as a protein kinase c substrate and a s100b-binding protein. *Proceedings of the National Academy of Sciences*, 89:11627–11631, 1992.

[118] RR Rustandi, AC Drohat, DM Baldisseri, PT Wilder, and DJ Weber. The Ca^{2+}-dependent interaction of s100b ($\beta\beta$) with a peptide derived from p53. *Biochemistry*, 37:1951–1960, 1998.

[119] C Delphin, M Ronjat, JC Deloulme, G Garin, L Debussche, Y Higashimoto, K Sakaguchi, and J Baudier. Calcium-dependent interaction of s100b with the c-terminal domain of the tumor suppressor p53. *Journal of Biological Chemistry*, 274:10539–10544, 1999.

[120] J Lin, Q Yang, Z Yan, J Markowitz, PT Wilder, F Carrier, and DJ Weber. Inhibiting s100b restores p53 levels in primary malignant melanoma cancer cells. *Journal of Biological Chemistry*, 279:34071–34077, 2004.

[121] J Lin, M Blake, C Tang, D Zimmer, RR Rustandi, DJ Weber, and F Carrier. Inhibition of p53 transcriptional activity by the s100b calcium-binding protein. *Journal of Biological Chemistry*, 276:35037–35041, 2001.

[122] PT Wilder, J Lin, CL Bair, TH Charpentier, D Yang, M Liriano, KM Varney, A Lee, AB Oppenheim, S Adhya, et al. Recognition of the tumor suppressor protein p53 and other protein targets by the calcium-binding protein s100b. *Biochimica et Biophysica Acta (BBA)-Molecular Cell Research*, 1763:1284–1297, 2006.

[123] J Lin, Q Yang, PT Wilder, F Carrier, and DJ Weber. The calcium-binding protein s100b down-regulates p53 and apoptosis in malignant melanoma. *Journal of Biological Chemistry*, 285:27487, 2010.

[124] J Van Dieck, MR Fernandez-Fernandez, DB Veprintsev, and AR Fersht. Modulation of the oligomerization state of p53 by differential binding of proteins of the s100 family to p53 monomers and tetramers. *Journal of Biological Chemistry*, 284:13804–13811, 2009.

[125] J van Dieck, DP Teufel, AM Jaulent, MR Fernandez-Fernandez, TJ Rutherford, A Wyslouch-Cieszynska, and AR Fersht. Posttranslational modifications affect the interaction of s100 proteins with tumor suppressor p53. *Journal of molecular biology*, 394:922–930, 2009.

[126] J Tian, AM Avalos, SY Mao, B Chen, K Senthil, H Wu, P Parroche, S Drabic, D Golenbock, C Sirois, et al. Toll-like receptor 9-dependent activation by dna-containing immune complexes is mediated by hmgb1 and rage. *Nature immunology*, 8:487–496, 2007.

[127] VV Orlova, EY Choi, C Xie, E Chavakis, A Bierhaus, E Ihanus, CM Ballantyne, CG Gahmberg, ME Bianchi, PP Nawroth, et al. A novel pathway of hmgb1-mediated inflammatory cell recruitment that requires mac-1-integrin. *The EMBO journal*, 26:1129–1139, 2007.

[128] A Taguchi, DC Blood, G del Toro, A Canet, DC Lee, W Qu, N Tanji, Y Lu, E Lalla, C Fu, et al. Blockade of rage–amphoterin signalling suppresses tumour growth and metastases. *Nature*, 405:354–360, 2000.

[129] SS Yan, ZY Wu, HP Zhang, G Furtado, X Chen, SF Yan, AM Schmidt, C Brown, A Stern, J Lafaille, et al. Suppression of experimental autoimmune encephalomyelitis by selective blockade of encephalitogenic t-cell infiltration of the central nervous system. *Nature medicine*, 9:287–293, 2003.

[130] Q Ding and JN Keller. Splice variants of the receptor for advanced glycosylation end products (rage) in human brain. *Neuroscience letters*, 373:67–72, 2005.

[131] R Businaro, S Leone, C Fabrizi, G Sorci, R Donato, GM Lauro, and L Fumagalli. S100b protects lan-5 neuroblastoma cells against aβ amyloid-induced neurotoxicity via rage engagement at low doses but increases aβ amyloid neurotoxicity at high doses. *Journal of neuroscience research*, 83:897–906, 2006.

[132] M Koch, S Chitayat, BM Dattilo, A Schiefner, J Diez, WJ Chazin, and G Fritz. Structural basis for ligand recognition and activation of rage. *Structure*, 18:1342–1352, 2010.

[133] CL Masters, G Simms, NA Weinman, G Multhaup, BL McDonald, and K Beyreuther. Amyloid plaque core protein in alzheimer disease and down syndrome. *Proceedings of the National Academy of Sciences*, 82:4245–4249, 1985.

[134] DJ Selkoe et al. Translating cell biology into therapeutic advances in alzheimer's disease. *NATURE-LONDON-*, 399:23–31, 1999.

[135] C Opazo, X Huang, RA Cherny, RD Moir, AE Roher, AR White, R Cappai, CL Masters, RE Tanzi, NC Inestrosa, et al. Metalloenzyme-like activity of alzheimer's disease β-amyloid. cu-dependent catalytic conversion of dopamine, cholesterol, and biological reducing agents to neurotoxic h(2)o(2). *Journal of Biological Chemistry*, 277:40302–40308, 2002.

[136] J Dong, CS Atwood, VE Anderson, SL Siedlak, MA Smith, G Perry, and PR Carey. Metal binding and oxidation of amyloid-β within isolated senile plaque cores: Raman microscopic evidence. *Biochemistry*, 42:2768–2773, 2003.

[137] J Steiner, B Bogerts, ML Schroeter, and HG Bernstein. S100b protein in neurodegenerative disorders. *Clinical Chemistry and Laboratory Medicine*, 49:409–424, 2011.

[138] E Roltsch, L Holcomb, KA Young, A Marks, and DB Zimmer. Psapp mice exhibit regionally selective reductions in gliosis and plaque deposition in response to s100b ablation. *Journal of Neuroinflammation*, 7:78, 2010.

[139] H Tamano and A Takeda. Dynamic action of neurometals at the synapse. *Metallomics*, 2011.

[140] K Yanamandra, O Alexeyev, V Zamotin, V Srivastava, A Shchukarev, AC Brorsson, GG Tartaglia, T Vogl, R Kayed, G Wingsle, et al. Amyloid formation by the pro-inflammatory s100a8/a9 proteins in the ageing prostate. *PLoS One*, 4:e5562, 2009.

[141] G Meloni, V Sonois, T Delaine, L Guilloreau, A Gillet, J Teissié, P Faller, and M Vašák. Metal swap between zn7-metallothionein-3 and amyloid-β–cu protects against amyloid-β toxicity. *Nature Chemical Biology*, 4:366–372, 2008.

[142] AI Bartlett and SE Radford. An expanding arsenal of experimental methods yields an explosion of insights into protein folding mechanisms. *Nature structural & molecular biology*, 16:582–588, 2009.

[143] NJ Greenfield. Using circular dichroism spectra to estimate protein secondary structure. *Nature protocols*, 1:2876, 2006.

[144] P Atkins and J de Paula, Atkins. *Elements of Physical Chemistry*. Oxford University Press, 2005.

[145] B Ranjbar and P Gill. Circular dichroism techniques: Biomolecular and nanostructural analyses-a review. *Chemical Biology & Drug Design*, 74:101–120, 2009.

[146] SM Kelly, TJ Jess, and NC Price. How to study proteins by circular dichroism. *Biochimica et Biophysica Acta (BBA)-Proteins & Proteomics*, 1751:119–139, 2005.

[147] A Hawe, M Sutter, and W Jiskoot. Extrinsic fluorescent dyes as tools for protein characterization. *Pharmaceutical research*, 25:1487–1499, 2008.

[148] CM Jones. An introduction to research in protein folding for undergraduates. *Journal of chemical education*, 74:1306, 1997.

[149] LA Munishkina and AL Fink. Fluorescence as a method to reveal structures and membrane-interactions of amyloidogenic proteins. *Biochimica et Biophysica Acta (BBA)-Biomembranes*, 1768:1862–1885, 2007.

[150] U Nobbmann, M Connah, B Fish, P Varley, C Gee, S Mulot, C Juntao, Z Liang, Lu Yanling, S Fei, et al. Dynamic light scattering as a relative tool for assessing the molecular integrity and stability of monoclonal antibodies. *Biotechnology & genetic engineering reviews*, 24:117–128, 2007.

[151] JS Philo. Is any measurement method optimal for all aggregate sizes and types? *The AAPS Journal*, 8:564–571, 2006.

[152] BJ Henriques, LM Saraiva, and CM Gomes. Combined spectroscopic and calorimetric characterisation of rubredoxin reversible thermal transition. *Journal of chemical education*, 2005.

[153] T Ostendorp, CW Heizmann, PMH Kroneck, and G Fritz. Purification, crystallization and preliminary x-ray diffraction studies on human Ca^{2+}-binding protein s100b. *Acta Crystallographica Section F: Structural Biology and Crystallization Communications*, 61:673–675, 2005.

[154] A Landar, TL Hall, EH Cornwall, JJ Correia, AC Drohat, DJ Weber, and DB Zimmer. The role of cysteine residues in s100b dimerization and regulation of target protein activity. *Biochimica et Biophysica Acta (BBA)-Protein Structure and Molecular Enzymology*, 1343:117–129, 1997.

[155] IS Matsui Lee, M Suzuki, N Hayashi, J Hu, LJ Van Eldik, K Titani, and M Nishikimi. Copper-dependent formation of disulfide-linked dimer of s100b protein. *Archives of Biochemistry and Biophysics*, 374:137–141, 2000.